Respirable Particulate Compliance Assessment

- Incremental PM_{10} due to Quarrying Activities (Roydon Quarry)

November 2024

PORTHILL

Submitted to:

Don Chittock

Fulton Hogan Limited

Christchurch

Submitted by:

Port Hill Limited

Document No: 2024-011-001-R Nov2024

Table of Contents

Appendices

Figures

Tables

1.0 Introduction

Fulton Hogan Limited (Fulton Hogan) operates a quarry at McDowell Drive in Templeton. This is referred to as Roydon Quarry (the site). Perimeter bund formation activities were carried out at this site from 6 June to 25 November 2022 around Madisons Rd, Curraghs Rd, Dawsons Rd and Jones Rd.

The site operates under Resource Consents CRC224104 issued by Canterbury Regional Council and RC185627 issued by Selwyn District Council. While consent RC185627 does not include any conditions relevant to dust management, Consent CRC224104 (the consent) includes a monitoring section (Conditions 12 to 21) detailing the meteorological and respirable particulate matter (PM_{10}) monitoring required to assess the air quality impacts of the consented activities.

Conditions 29 to 31 outline the reporting requirements relating to PM_{10} offsets, including in Condition 29, the requirement to:

"...obtain reports from a SQEP in air quality assessing compliance with Regulation 17(1) of the Resource Management (National Environmental Standards for Air Quality) Regulations 2004..."

To meet Condition 29, this report provides an analysis of ambient monitoring data, and an assessment of compliance with Regulation 17 of the National Environmental Standards (NES). This investigates the likelihood of there being an exceedance of the maximum incremental rise of 2.5 $\mu g/m^3$ 24-hour PM_{10} concentration occurred within the nearby Christchurch airshed, due to the site's quarrying activities.

The definition of "quarry activities" is provided in General Condition 2(a) of the consent as being the activities listed in General Condition 1(a) to (i) as follows:

a) Site preparation, topsoil stripping, overburden removal and storage;

b) Construction and maintenance of bunds and stockpiles;

c) Extraction, loading and transportation of material;

d) Processing of aggregates (including crushing and screening of aggregates);

e) Combustion products from the operation of 1.04 megawatt of diesel fired generation (up to 4 generators);

f) Stockpiling of aggregates;

g) Deposition of clean fill;

h) Site rehabilitation; and

i) Movement of vehicles associated with the above activities.

This report provides a summary of the data collected, methodology used and subsequent independent assessment to investigate whether, or not, the site was likely to have complied with Regulation 17 during the period of bund formation.

2.0 Ambient Monitoring

In accordance with Condition 18 of the consent, a USEPA-certified reference-grade ambient PM_{10} monitor (Teledyne, Model T640x) has been operated since December 2021at the site's eastern boundary, which is adjacent with the boundary of Christchurch airshed. This continuously records 1-minute average ambient PM_{10} and $PM_{2.5}$ concentrations.

Condition 19 of the consent requires pre-calibrated real-time PM_{10} monitors to be located at, or near to the quarry's southeast, southwest and northwest boundaries.

Condition 19.e., allows the use of monitors which do not meet the standard for PM_{10} compliance monitors as specified under the National Environmental Standard for Air Quality – PM_{10} (NESAQ-PM_{10}). The monitors selected were the QuantAQ Modulairs (QuantAQs). It is understood that the QuantAQ monitors were selected by Fulton Hogan in consultation with industry experts and Canterbury Regional Council.

Five QuantAQ ambient PM_{10} monitors were co-located and operated in parallel with the T640x monitor to enable their calibration as required by Condition 19.e.ii. Following the calibration period and prior to the commencement of any quarry activities (including bund formation works) at the site, three monitors were positioned around the site boundary at the locations specified in Condition 19.a i, ii and iii, and one QuantAQ monitor remained collocated with the T640x. The remaining monitoring was retained as a backup but was not operated during the background monitoring or bund formation period and therefore was not evaluated further.

The site also has a 6 m high meteorological monitoring station installed by Scott Technology to comply with Conditions 12 to 17.

For this report, the following raw ambient monitoring data and site information was evaluated:

- 1-minute average PM_{10} and $PM_{2.5}$ concentrations recorded by a USEPA certified monitor T640x, manufactured by Teledyne.
- Calibration certificates for the T640x in February and May 2022, and from July to November 2022.
- 15-minute average wind, temperature, and relative humidity measured by a Scott Met Station (Wind measured at a height of six metres).
- 1-minute average PM_{10} and $PM_{2.5}$ concentrations, relative humidity, temperature measured by four QuantAQ monitors (Q1, Q2, Q3, Q4).
- Site diary notes providing work dates, notes related to on-site activities (including quarrying related, or other agricultural/paddock work), weather conditions, crews working, and miscellaneous notes.
- Timelapse footage from an on-site camera, situated just north of the Central Processing Stockpiling Area (CPSA – shown in green in Figure 2.1.

The locations of all ambient PM_{10} monitors are shown in Figure 2.1.

A summary of ambient monitoring data made available for this assessment is provided in Table 2.1

Table 2.1: Summary of data used in this assessment.

Monitor	Deployment location	Start Date	End Date
T640x	Dawsons Rd	22 Dec 2021	5 Dec 2022
Scott Met Station	On site	22 Dec 2021	5 Dec 2022
Q1	Co-located with T640x Dawsons Rd	9 Feb 2022	5 Dec 2022
Q2, Q3, Q4	Co-located with T640x (calibration period)	9 Feb 2022	5 May 2022
Q2	Intersection of Jones Rd and Dawsons Rd	5 May 2022	5 Dec 2022
Q3	Maddisons Rd	5 May 2022	5 Dec 2022
Q4	Intersection of Jones Rd and Curraghs Rd	5 May 2022	5 Dec 2022

LEGEND

- Monitor Locations
- Meteorological Station
- Central Processing Stockpilling Area (CPSA)
- Site Boundary
- Christchurch Airshed

CONSULTANT

PORTHILL

NOTES

1. Aerial: Image © 2024 Google Earth, accessed 1 November 2024
2. Schematic only, not to be interpreted as an engineering desgin or construction drawing.
3. Reference Scale: 1:17,500

0 400 800 m

CLIENT AND PROJECT

Fulton Hogan Limited
Respirable Particulate Compliance Assessment

TITLE

Monitor Locations During Bund Formation Activities

DOCUMENT NUMBER	FIGURE	DRAWN	APPROVED	DATE
2024-011-001	**2.1**	IX	CN	7/11/2024

3.0 Pre-Processing Raw Data

The raw T640x and weather data from the Scott Technology weather station required minimal pre-processing as these data are produced from calibrated instruments. For this data only periods when calibration was being undertaken were removed.

While the T640x is not a certified NES reference method it is a USEPA-certified reference-grade ambient PM_{10} monitor and local colocation studies (Aberkane, 2019) indicate it performs well (with slightly elevated measurements) relative to instruments that are used as reference methods and has therefore is considered appropriate for this study and the data treated as NES equivalent.

For the QuantAQs, raw measurement preprocessing for data quality was required in a two stage process. The first stage was to remove 1-minute PM_{10} concentration records which were > 2000 $\mu g/m^3$ or when the relative humidity was > 95%. This is due to these values being outside the instrument operational range (Quant Modulair-PM Product Specification Sheet, 2022).

The second round of raw data removal was based on the identification of fog events which often leads to an overestimation of PM_{10} readings in QuantAQs (McClosky & Hagan, 2024). This is described in Appendix A.

Following data removal for quality, Hourly and daily averages were determined. When determining hourly and daily averages, when data capture was less than 75% in the averaging period being considered, an average value was not calculated. This approach is consistent with Ministry for Environment data quality assurance methods (Ministry for the Environment, 2009). Daily (24 hour averages) were calculated based on midnight to midnight time period and reported at midnight each day consistent with the requirements of the NES.

Plots of data collected during the colocation periods and a summary of the methods, data capture and removal percentages from the raw data sets are provided in Appendix A.

4.0 Methodology

4.1 General

This compliance assessment requires the difference in 24-hour average PM_{10}, as measured between monitors located along western and southwestern boundaries of the site, to be compared with those located at the eastern boundary of the site (adjacent to the Christchurch airshed boundary). Non-compliance would occur if a statistically significant increase in 24-hour average PM_{10} (midnight to midnight) by 2.5 $\mu g/m^3$, or higher, is detected, and can be linked to quarrying activities at the site. Therefore, the monitoring to establish the site's level of compliance required the following steps:

1. The calibration of the QuantAQ boundary monitors for 24-hour PM_{10} using best fit regression equations for measurements produced by the monitors versus measurements produced by a co-located Teledyne, Model T640x PM_{10} monitor (T640x) - a US EPA reference method. Both orthogonal and linear regressions were undertaken between 24-hour PM_{10} measured by each QuantAQ monitor (Q1, Q2, Q3, and Q4) and the values measured concurrently by the T640x reference monitor.
2. Use of regression equations (both linear and orthogonal) as established for each QuantAQ monitor, to adjust/correct their raw 24-hour PM_{10} values so these are made as equivalent, as possible, to the T640x measurements.

3. Use of the adjusted 24-hour PM_{10} values recorded by each QuantAQ monitor (by applying their respective regression equations to raw data) to established mean absolute error (MAE) values for each QuantAQ unit with respect to the T640x reference method.
4. Use of adjusted 24-hour PM_{10} values recorded by each QuantAQ monitor to establish a distribution of 24-hour PM_{10} $\mu g/m^3$ differences during the co-location period including Q1-Q2, Q1-Q3 and Q1-Q4.
5. Use individual errors for each QuantAQ with respect to the T640x unit for 24-hour PM_{10}, to establish combined errors for observed differences between airshed boundary and other boundary monitors; namely Q1-Q2, Q1-Q3 and Q1-Q4.
6. Undertake statistical analysis of distributions of 24-hour PM_{10} differences for Q1-Q2, Q1-Q3 and Q1-Q4 including tests for normality or skewness and use appropriate methods for either normal or skewed distributions to calculate 90th percentile upper limit for each distribution of 24-hour PM_{10} differences.
7. Use the above results of each of the combined error and upper confidence limits for differences in 24-hour PM_{10} between Q1 and other monitors, assess the likelihood that a statistical significant increase in 24-hour PM_{10} occurred across the site on any day during the monitoring period.
8. For all days, where a statistically significant increases in 24-hour PM_{10} across the site is detected, then investigate whether or not, other onsite or offsite activities (e.g. agricultural activities onsite) were likely to be significant sources of increased 24-hour PM_{10}, or if quarry activities were the likely source.

The last step in the above assessment was aided by site diary records for each day, satellite and site imagery, and plotted distributions of hourly PM_{10} concentration versus wind direction and frequency (i.e., PM_{10} concentration roses).

The specific details of error analysis and use of statistical tests are discussed in the following section, suffice to say, that multiple test methods have been applied to establish any days where the 24-hour PM_{10} at the eastern site boundary (adjacent to the Christchurch airshed boundary) has a statistically significant increase of > 2.5 $\mu g/m^3$ compared to monitoring locations along the western and southern boundaries of the site.

These statistical tests involve either a consideration of the combined instrumental error for calculated 24-hour PM_{10} differences, as well as upper confidence intervals for the distribution (i.e., the noise inherent in calculated differences in 24-hour PM_{10} between Q1 and other monitors (Q2, Q3 and Q4).

The various methods discussed above, have been employed to provide multiple alternative approaches for detecting an increase in 24-hour PM_{10} at the Christchurch airshed boundary, which is statistically significant and at least 2.5 $\mu g/m^3$ above the random noise inherent in the PM_{10} monitors. The co-location study was critical for enabling this instrument noise and combined instrument errors to be established.

4.2 Co-location study results

The 3 month co-location study period (9 February to 5 May 2022 for Q2, Q3 and Q4 and T640x) provided the essential data for establishing regressions between the T640x and QuantAQ monitors. For Q1, the co-location with the T640x was for the entire 11 month study period.

Regression analysis

The primary method adopted is an orthogonal regression of 24-hour PM_{10} measured by the QuantAQs against values by the T640x monitor. Both the T640x and QuantAQ monitors have error in their measured 24-hour PM_{10} values. In such cases, an orthogonal regression is expected to provide a more accurate regression line compared to a linear regression. This regression method is also recommended in standard methods for confirming the equivalency of PM_{10} monitoring devices with NES certified methods[1], and is further discussed by (Aberkane, 2019).

Notwithstanding the above, a linear regression was also applied to 24-hour PM_{10} values recorded by the QuantAQ and T640x during the co-location period. This regression was improved slightly by including relative humidity as a variable.

Both results of orthogonal and linear regressions of the QuantAQ monitors versus the T640x for 24-hour PM_{10} values are summarised in Appendix B and both approaches were used in this report. Because Q1 was co-located with the T640x for 11 months (see Table 2.1), then this larger data set was used for the regression of Q1 measurements of 24-hour PM_{10} versus the T640x's concurrent measurements. Regressions for the other QuantAQ devices versus the T640x were based on the 3-month co-location period.

Instrument error analysis

The residual instrument error for each QuantAQ was defined as the Mean Absolute Error (MAE), which was established from the population of differences between the T640x 24-hour PM_{10} values and those measured by each QuantAQ following adjustment of values using each of the orthogonal and linear regression equations.

The MAE is the average difference between all QuantAQs 24-hour PM_{10} values and those measured by the T640x during each day of the co-location period. Therefore, for each QuantAQ, the absolute error for any one day is the difference between the adjusted 24-hour PM_{10} and the T640x value for that day. This is repeated for all days of the co-location periods where there is valid data, and the average value for each QuantAQ is it's MAE value.

MAE values are provided in Appendix C for both the linear and orthogonal regressions and are summarised in Table 4.1.

Table 4.1 Mean Absolute Error - 24-hour PM_{10} (QuantAQ Monitors)

QuantAQ Monitors	Orthogonal regression	Linear regression
	MAE (µg/m^3)	MAE (µg/m^3)
Q1	3.4	4.8
Q2	3.1	4.0
Q3	2.5	2.6
Q4	2.5	2.5

Using the MAE values in Table 4-1 for each of the QuantAQ monitors (i.e., with respect to the T640x monitor's 24-hour PM_{10} values), the combined error for 24-hour PM_{10} differences between the QuantAQ monitors was calculated using the square root of the sum of the squared errors. The resultant combined errors are shown in Table 4.2. For each of the regression methods, these MAE values provide a lower limit of data reliability relative to the T640x and therefore only differences observed above the

[1] AS/NZS 3580.9.17:2018 Demonstration of equivalence for ambient particulate matter monitoring methods

combined MAE values are considered reliable to determine a difference in concentration relative to the criteria. As the combined difference MAE values are all above 2.5 µg/m^3, this means any observed differences needs to be greater than the MAE value to be considered reliable.

Table 4.2 Combined Difference Error - 24-hour PM10 (QuantAQ Monitors)

QuantAQ Monitors	Orthogonal regression	Linear regression
	MAE (µg/m^3)	MAE (µg/m^3)
Q1-Q2	4.6	6.3
Q1-Q3	4.2	5.5
Q1-Q4	4.2	5.4

Difference distributions & confidence intervals

The distribution of differences in 24-hour PM_{10} values measured by Q1 versus the other QuantAQ monitors during the co-location study was calculated following adjustments (using both the linear and orthogonal regressions to correct raw data) to each monitors' 24-hour average PM_{10} values. It can be noted that the distribution of these differences indicates the random noise and consistent biases between instruments that produces both negative and positive differences in 24-hour PM_{10} when all the monitors are exposed to the exact same ambient 24-hour PM_{10} levels.

The resultant distributions of 24-hour PM_{10} differences are summarised in Appendix C. This details the statistical tests which confirm the non-normality or normality of the difference distributions (tested via the Shapiro-Wilk test and Kologorov-Smirnov tests methods). Upper confidence limits based on the data values 90th percentile of the data was calculated. These were very similar to confidence intervals calculated standard z-statistic for normal distributions and lower than those calculated based on the Bootstrap method which does not rely on data being normally distributed. The analysis has proceeded based on the 90th percentile values as being representative of the 90th percentile upper confidence limit.

The mean values for each distribution and 90th percentile upper confidence limits and provided below in Table 4.3.

Table 4.3 Distribution of 24-hour PM_{10} differences (Co-location study)

QuantAQ Monitors	Orthogonal regression		Linear regression	
	90th confidence (µg/m^3)	Mean diff. (µg/m^3)	90th confidence (µg/m^3)	Mean diff. (µg/m^3)
Q1-Q2	-1.5 to 6.4	2.8	-5 to 11	4.0
Q1-Q3	-0.5 to 2.6	0.9	-3 to 3	-0.1
Q1-Q4	-0.7 to 5.9	2.2	-4 to 11	3.0

4.3 Assessment of results

For each day of the boundary monitoring period (5 May to 5 December 2022), the adjusted values of 24-hour PM_{10} (µg/m^3) measured by Q1, Q2, Q3 and Q4 were compared. From the differences between the monitors, days were identified where Q1's 24-hour PM_{10} value (adjacent to the airshed boundary) was higher than one or more of the quarry boundary monitors (Q3 at the northwest boundary, Q4 at the southwest boundary and Q2 at the southeastern site boundary) and by an extent that exceeded relevant MAE combined errors (Table 4.2), or was else 2.5 µg/m^3, or more higher than the 90% percentile confidence limit (Table 4.3) established for differences in 24-hour PM_{10} measured between monitors and which is associated with instrument error.

The days identified with statistically significant increases in 24-hour PM_{10} ($\mu g/m^3$) adjacent to the airshed boundary compared to other site boundaries, were further evaluated to assess the likely source, including the quarry, or else non-quarrying activities occurring on, or off the site. As such, information was established for days of significant increases in 24-hour PM_{10} ($\mu g/m^3$) adjacent to the airshed boundary compared to other site boundary locations, as follows:

1. The presence or absence of quarrying activity on the day
2. The presence or absence of other onsite activities, which were likely to discharge significant levels of PM_{10} on the day
3. Polar plots of hourly PM10 concentrations for each QuantAQ monitor (and including the T640x), which showed their magnitude as a function of wind direction and frequency throughout the day. Note all polar plots are based on uncorrected hourly data and therefore should only be used to provide direction of impacts and indicative scale of PM10 concentrations.
4. Review the hourly measurements of key monitors to confirm no missing data for hours when other monitors show elevated PM_{10}.
5. Review meteorological conditions and time of day (operational vs non-operational hours) to assess the likelihood of high humidity and low wind speed being the primary cause of elevated PM_{10}.

The above information enabled an assessment of whether quarry, other onsite activities, or else off-site source of ambient PM_{10} were the likely cause of increased 24-hour PM_{10} being detected opposite the Christchurch airshed boundary.

5.0 Findings

The key results of the analysis of all monitoring days (via the method described in Section 4.3) are summarised in Table 5.1. The days identified are when monitors located along the southern, northern and western boundaries (Q2, Q3 and Q4) of the site, measured a significantly lower 24-hour PM_{10} concentration than the monitor located adjacent to the airshed boundary (Q1).

The information in Table 5.1 highlights which of the boundary monitors measured 24-hour PM_{10} that was lower by more than 2.5 µg/m^3 than Q1's value for the day, and which statistical test methods detected this difference as being statistically significant (i.e., not likely to be explained by instrumental random error).

There were eight days, where this occurred, which were further investigated to confirm if the site's quarrying activities were the likely cause of higher PM_{10} levels measured by Q1. Note all polar plots are based on uncorrected hourly data and therefore should only be used to provide direction of impacts and indicative scale of PM_{10} concentrations.

Table 5.1 Days when increase in 24-hour PM10 exceeds significance criteria and the relevant QuantAQ monitors to the west or south of Q1.

Date	Orthogonal regression		Linear regression		Onsite agriculture activities (Y/N)
	Difference > MAE	Difference > 90th % CI + 2.5 µg/m^3	Difference > MAE	Difference > 90th% CI + 2.5 µg/m^3	
7/07/2022	Q2	-	Q2 & Q4	-	N
27/09/2022	Q2	-	Q2	-	N
4/11/2022	Q3 & Q4	Q3	Q2 & Q3 & Q4	Q3	Y
5/11/2022	-	-	Q4	-	N
6/11/2022	Q3	Q3	Q2 & Q3 & Q4	Q3	N
7/11/2022	Q2 & Q3 & Q4	Q3 & Q4	Q2 & Q3 & Q4	Q3 & Q4	N
8/11/2022	-	-	Q2 & Q4	-	N
10/11/2022	Q3	-	Q3 & Q4	Q3	N

Note: A dash (-) is indicative that there is no exceedance identified based on this criterion.

5.1 Day 1 - 7/07/2022

On the 7th July 2022, the MAE method indicated significant PM_{10} increases adjacent to the airshed boundary (Q1). This is due to measurements at Q2 (orthogonal and linear regression-based data corrections) and Q4 (for linear regression-based data corrections). However, the PM_{10} difference between monitors were not significantly higher than the random scatter of inter-instrument PM_{10} differences (for either orthogonal or linear regression-based data corrections).

The polar plots shown in Figure 5.1indicate that on this day, an apparent increase in PM_{10} between the southern boundary of the site (Q2) and Q1. On investigation into Q2 hourly data it was found it had seven hours of data removed (because of fog events) and these included the times when all other monitors measured the highest hourly PM_{10} levels (7 pm and to a lesser extent 8 pm). Therefore, for this day, it is necessary to consider the polar plot for Q4 and compare to Q1. This indicates significant sources of PM_{10} coming from offsite and from southeast and south directions. Given the meteorological conditions associated with all the elevated PM_{10} were associated with high humidity and low wind speeds outside of operational hours, then it is almost certain that the elevated PM_{10} on this day was due to fog/mist and that removal of data from Q2 and not these other monitors explain the apparent significant differences (i.e., a false positive statistical result).

Given the above and finding that PM_{10} differences were not significantly higher than the random scatter of inter-instrument PM_{10} differences, then it is concluded that the quarry emissions did not result in an increase in PM_{10} of more than 2.5 µg/m^3 (24-hour average) on 7th July 2022.

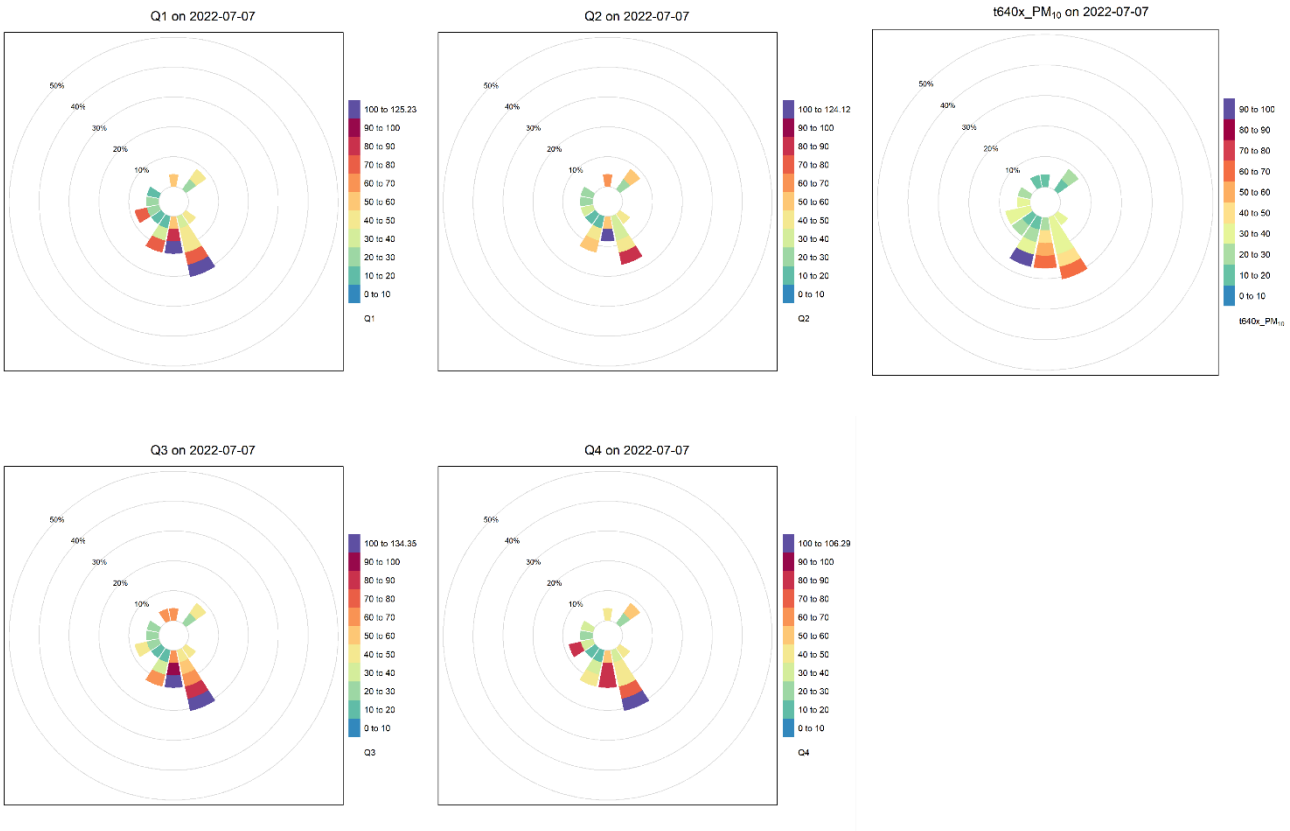

Figure 5.1: Polar plots for 1-hour Q1, Q2, Q3, Q4, T640x PM_{10} on 7/07/2022.

5.2 Day 2 - 27/09/2022

On the 27th September 2022, the MAE method indicated significant PM_{10} increases adjacent to the airshed boundary (Q1) compared to measurements at Q2 (orthogonal and linear regression-based data corrections). However, the PM_{10} difference between monitors was not detected as significant above the random scatter of inter instrument PM_{10} differences (for either orthogonal or linear regression-based data corrections).

The polar plots shown in Figure 5-2 indicate that on this day, an apparent increase in PM_{10} between the southern boundary of the site (Q2) and Q1 was due to an offsite source of PM_{10} levels that came from the north of the site. This is confirmed by the T640x and Q3 monitors. Given this finding then it is concluded that the quarry emissions did not result in an increase in PM_{10} of more than 2.5 µg/m^3 (24-hour average) on 27th September 2022.

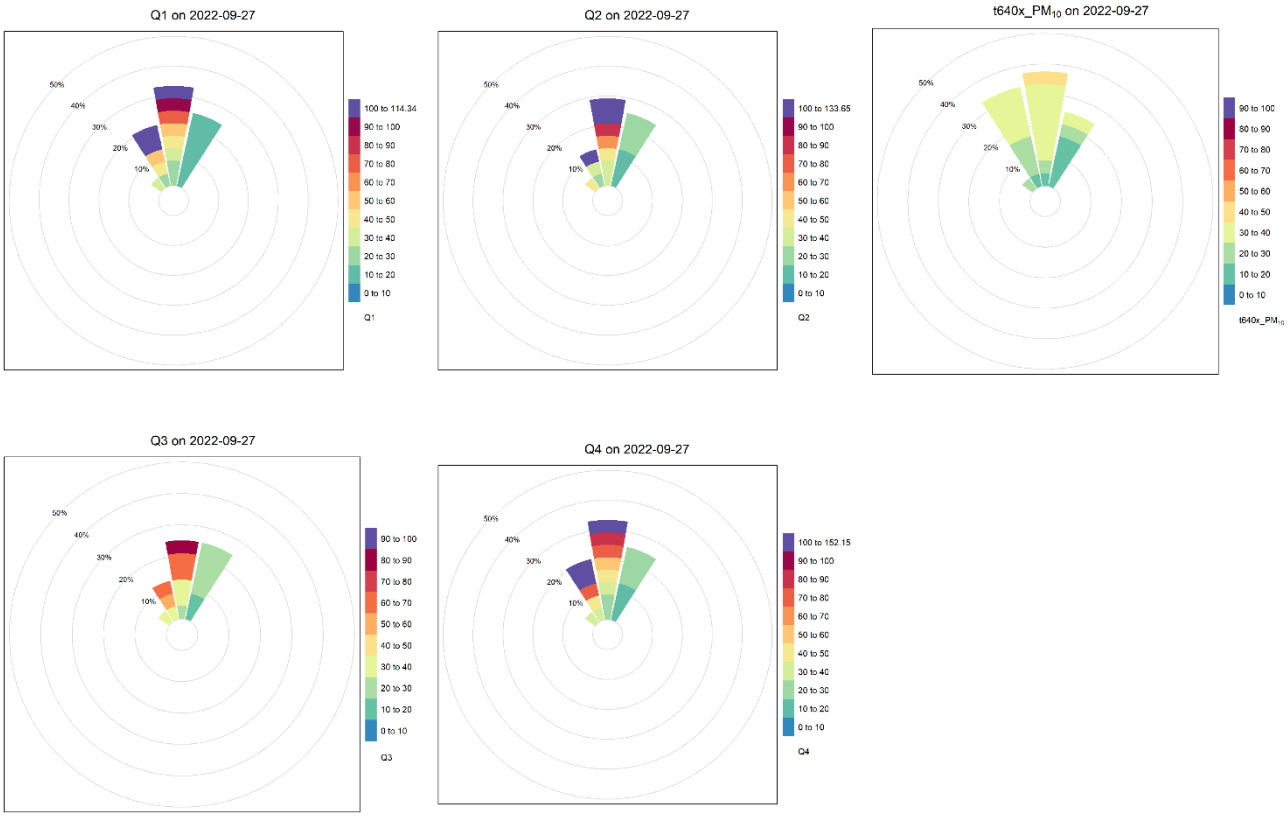

Figure 5.2: Polar plots for 1-hour Q1, Q2, Q3, Q4, T640x PM_{10} on 27/09/2022.

5.3 Day 3 - 4/11/2022

On the 4th November 2022, the MAE method indicated significant PM_{10} increases adjacent to the airshed boundary (Q1) compared to measurements at Q3 and Q4 (orthogonal and linear regression-based data corrections) and Q2 (linear regression). The PM_{10} difference between Q1 and Q3 was also detected as significant above the random scatter of inter instrument PM_{10} differences (for either orthogonal or linear regression-based data corrections). On this day, agricultural activity (paddock work) was occurring on the site, which is very likely to be a significant source of PM_{10} emission affecting Q1 and the T640x. Further to this, an analysis of the polar plots for PM_{10} measurements at each monitor indicate that offsite sources of PM_{10} to the west of the site were also likely to have contributed to elevated PM_{10} measurements at Q1 and the T640x

The polar plots shown in Figure 5-3 indicate that on this day, that elevated levels of PM_{10} were shown by Q4 to be coming from offsite and from the west to northwest direction. This monitor is downwind of paddocks during these wind conditions, and which have large exposed areas which would be prone to wind erosion of dust.

Given the presence on onsite paddock work on the 4th November 2022 and clear evidence of PM_{10} arriving from offsite and from the west to northwest direction, then it is not possible to conclude with any certainty that the quarry PM_{10}emissions did not comply with the site's consent on this day.

Whilst Q1 measured a 24-hour average PM_{10} concentration that was 2.5 µg/m^3 or higher than measured at the northwest boundary on this day, it is concluded that much of this difference in PM_{10} concentration was likely to have been caused by both onsite and offsite agricultural activity.

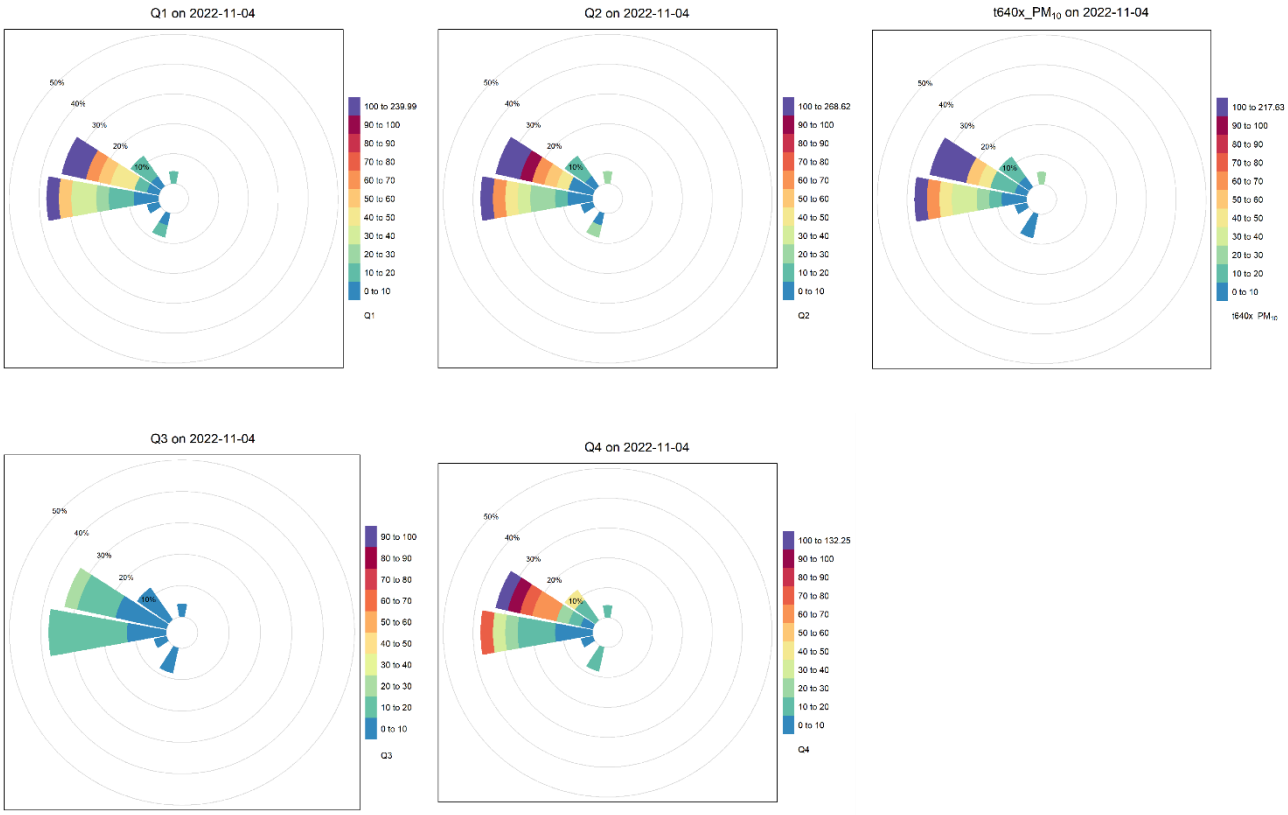

Figure 5.3: Polar plots for 1-hour Q1, Q2, Q3, Q4, T640x PM_{10} on 4/11/2022.

5.4 Day 4 - 5/11/2022

On the 5th November 2022, the MAE method indicated significant PM_{10} increases adjacent to the airshed boundary (Q1) compared to measurements at Q4 (only for linear regression-based data corrections). However, the PM_{10} difference with Q4 was not detected by the MAE based on orthogonal regression adjusted data, nor was it detected as significant above the random scatter of inter instrument PM_{10} differences (for either orthogonal or linear regression-based data corrections).

The polar plots shown in Figure 5-4 make it clear that the increase in PM_{10} between the southwestern boundary of the site (Q4) and Q1 was due to an offsite source of PM_{10} that came from the northeast of the site – there is also some small contribution from the northwest. Therefore, it is concluded that the

quarry emissions quarry emissions did not result in an increase in PM_{10} of more than 2.5 µg/m^3 (24-hour average) on 5th November 2022.

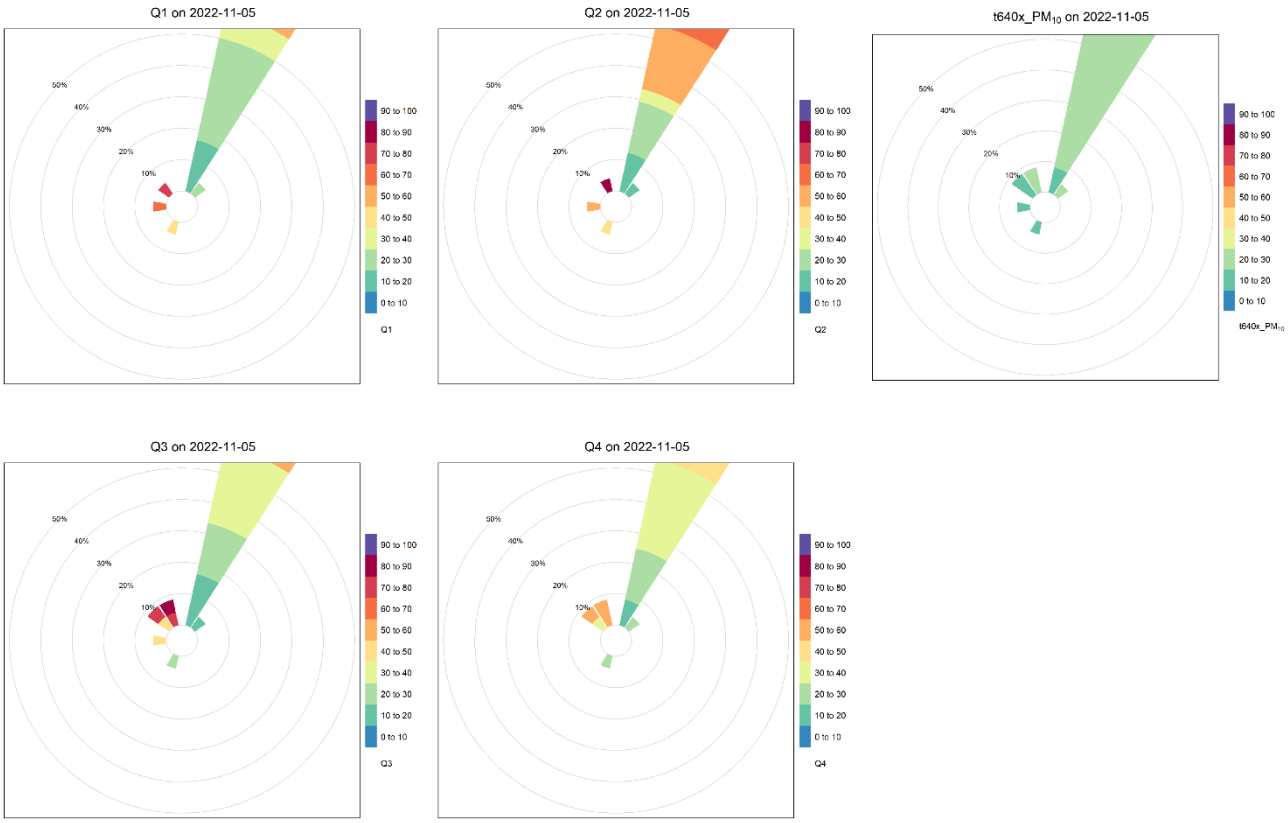

Figure 5.4: Polar plots for 1-hour Q1, Q2, Q3, Q4, T640x PM_{10} on 5/11/2022.

5.5 Day 5 - 6/11/2022

On the 6th November 2022, the MAE method indicated significant PM_{10} increases adjacent to the airshed boundary (Q1) compared to measurements at Q2, Q3 and Q4 (orthogonal and linear regression-based data corrections) and Q3 (orthogonal regression-based data corrections). The PM_{10} difference between Q1 and Q3 was also detected as significant above the random scatter of inter instrument PM_{10} differences (for either orthogonal or linear regression-based data corrections).

The polar plots shown in Figure 5-5 indicate that on this day, elevated levels of PM_{10} were shown by all monitors to be coming from offsite and from the northeast direction. It appears that Q1 was more impacted by this offsite source than Q3 and to an extent that the difference in measured was detected by most statistical tests. It is therefore concluded that the quarry emissions did not result in an increase in PM_{10} of more than 2.5 µg/m^3 (24-hour average) on 6th November 2022.

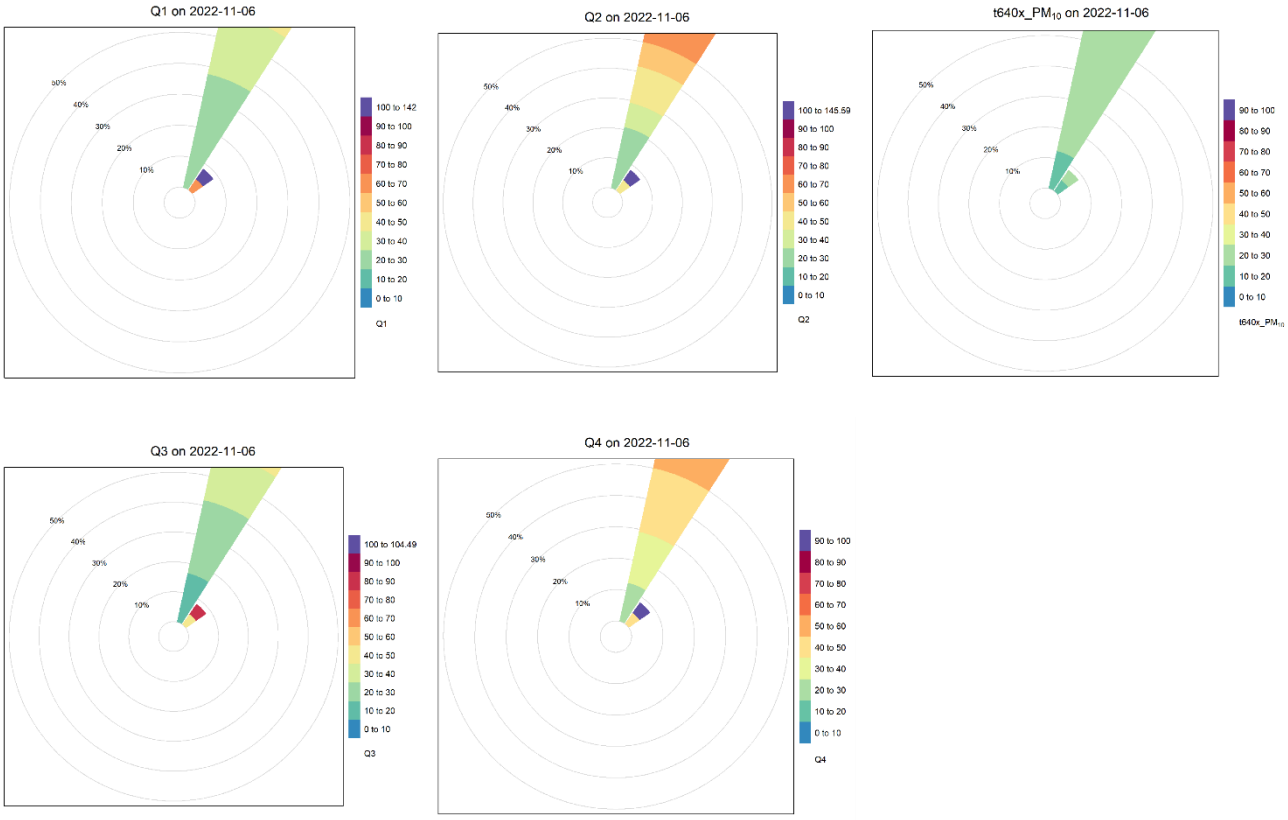

Figure 5.5: Polar plots for 1-hour Q1, Q2, Q3, Q4, T640x PM_{10} on 6/11/2022.

5.6 Day 6 - 7/11/2022

On the 7th November 2022, the MAE method indicated significant PM_{10} increases adjacent to the airshed boundary (Q1) compared to measurements at Q2, Q3 and Q4 (orthogonal and linear regression-based data corrections). The PM_{10} difference between Q1 compared to measurements at Q3 and Q4 were also detected as significant above the random scatter of inter instrument PM_{10} differences (for both orthogonal or linear regression-based data corrections).

As with the 7th of July 2022, an analysis of hours of day for elevated PM_{10} concentrations and associated meteorological conditions, make it clear that fog conditions are the most likely cause of the apparent significant differences in PM_{10} levels. Furthermore, that the primary source of real PM_{10} measured at the site, resultant from an offsite source from the southeast.

The polar plots shown in Figure 5-6 indicate that on this day, that elevated levels of PM_{10} were shown by monitors Q1, Q2 and Q3 to be coming from the north-northwest direction (that is mainly offsite) and 5 am to 7 am when the ambient conditions are humid, cool and wind is light. This is indicative of fog conditions which is confirmed by the T640x not measuring elevated PM_{10} concentrations from this direction and during this time. Therefore, the significant difference in PM_{10} concentrations between Q3 and Q1 are most certainly a result of fog effects and fog drifting from an offsite direction.

With regards to the elevated PM_{10} concentrations measured at Q1 compared to lower values at Q2 and Q4, the polar plots in Figure 5-6 confirm that Q2 and q4 were rarely, if ever upwind of Q1 on this day. However, both Q1 and Q2 were impacted in the late morning (11 am) by elevated PM_{10} concentrations which came from an offsite source located to the southeast of the site.

It is concluded that the quarry emissions did not result in an increase in PM_{10} of more than 2.5 µg/m^3 (24-hour average) on 7th November 2022 and that apparent increases in PM_{10} concentrations at the airshed boundary was due to offsite sources to the southeast, or other fog drifting from offsite during drainage flow conditions.

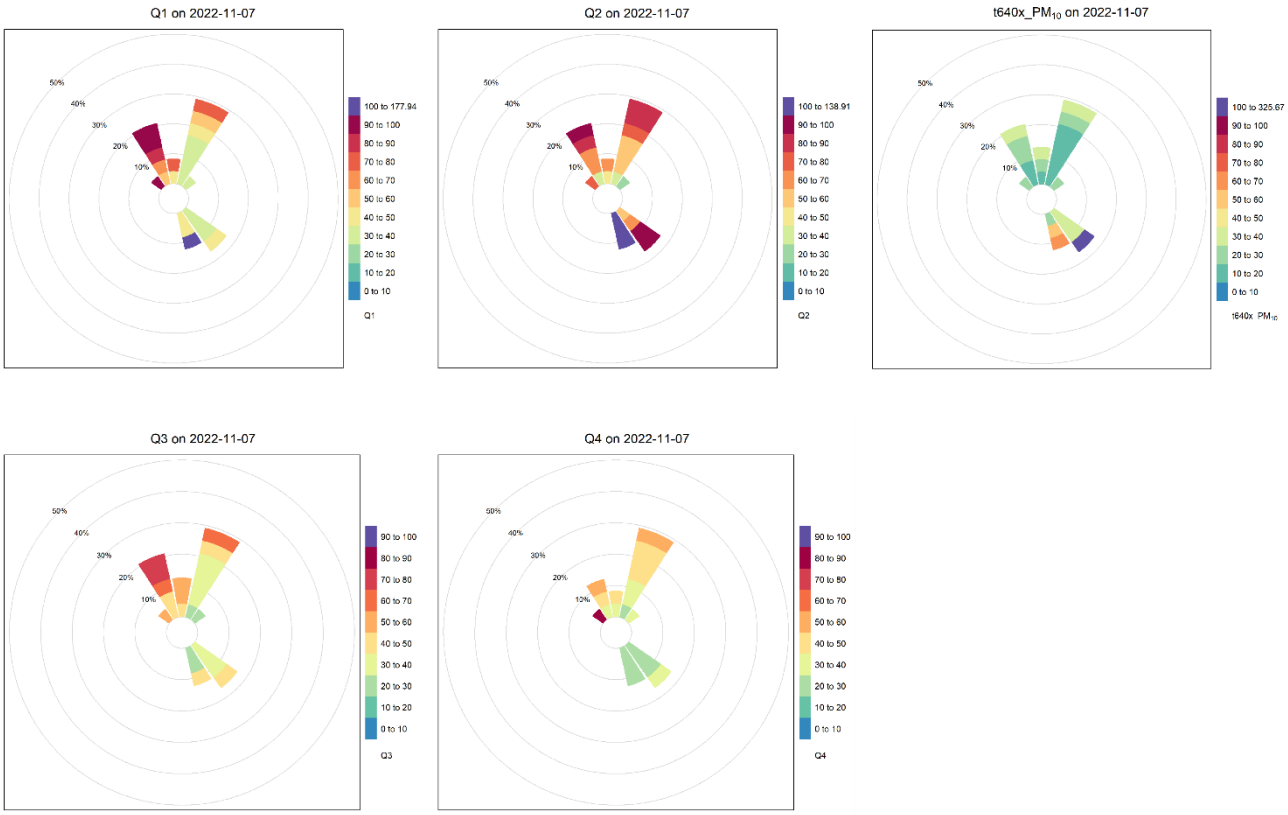

Figure 5.6: Polar plots for 1-hour Q1, Q2, Q3, Q4, T640x PM_{10} on 7/11/2022.

5.7 Day 7 - 8/11/2022

On the 8th November 2022, the MAE method indicated significant PM_{10} increases adjacent to the airshed boundary (Q1) compared to measurements at Q2 and Q4 (only for linear regression-based data corrections). However, the PM_{10} differences with Q2 and Q4 was not detected by the MAE based on orthogonal regression adjusted data, nor was it detected as significant above the random scatter of inter instrument PM_{10} differences (for either orthogonal or linear regression-based data corrections).

The polar plots shown in Figure 5-7 indicate increase in PM_{10} concentration at Q1 compared to the southwestern (Q4) and the southern site boundary (Q2) boundary. This absence of any PM_{10} concentration coming from the southwest direction at Q2 is indicative of data being removed for fog events. When investigating the hourly data for this day, it transpires that Q2 and Q4 respectively had 6 hours and 5 hours of high hourly PM_{10} values removed because of suspected fog events which occurred between 1 am and 6 am on this day. By comparison, the fog detection routine only removed 1 hour of elevated hourly PM_{10} from Q1.

Given the above, it is concluded that the significant differences between the 24-hour PM_{10} concentration measured at Q1versus Q2 and Q4, were an artifact of the imperfect routine for removing data based on suspected fog events and causing a bias towards Q1's PM_{10} recording by retaining more

of the elevated hours of data during cool humid conditions for this monitor. This is the same type of false positive error that was found to occur on the 7th July 2022.

It is concluded that the quarry emissions did not result in an increase in PM_{10} of more than 2.5 µg/m^3 (24-hour average) on 8th November 2022 and that apparent increases in PM_{10} concentrations at the airshed boundary was due to fog events producing concentrations which were not removed evenly from all QuantAQ monitors.

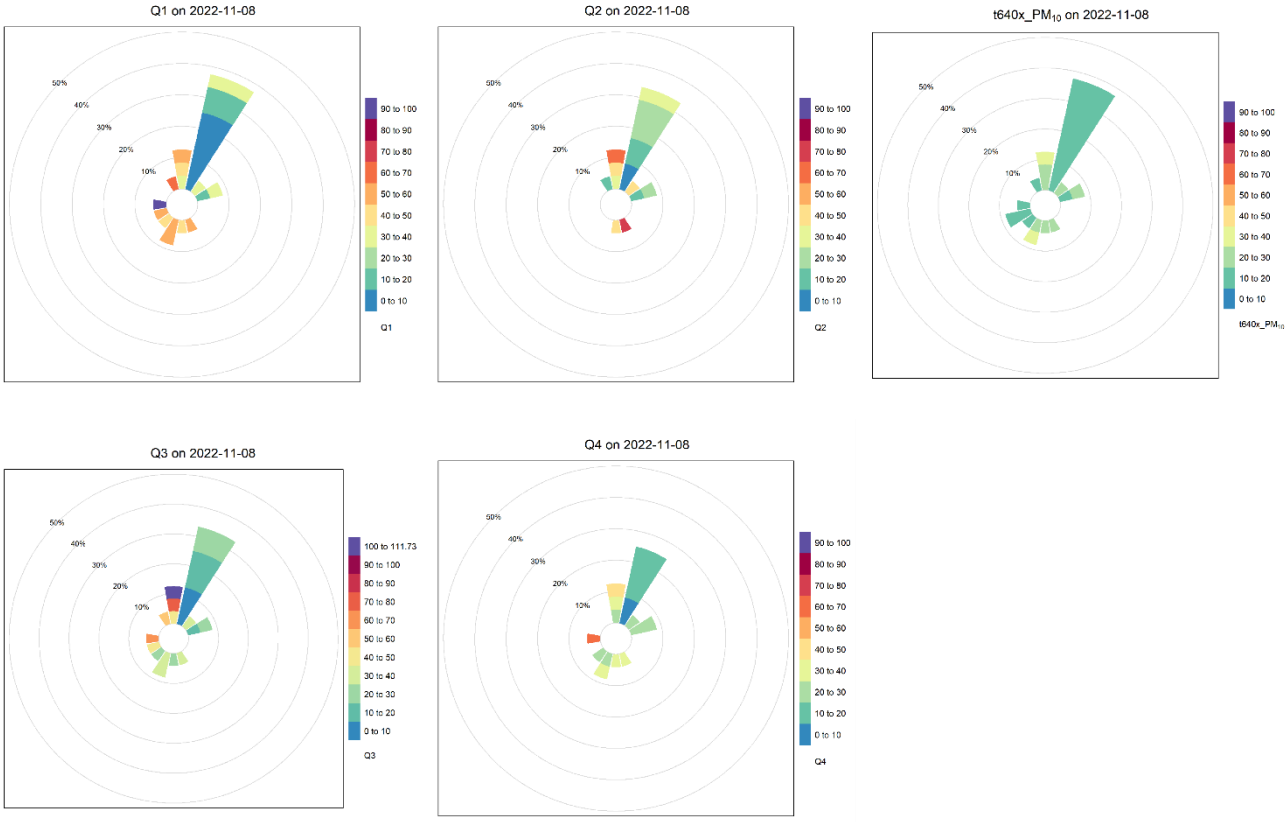

Figure 5.7: Polar plots for 1-hour Q1, Q2, Q3, Q4, T640x PM_{10} on 8/11/2022.

5.8 Day 8 - 10/11/2022

On the 10th November 2022, the MAE method indicated significant PM_{10} increases adjacent to the airshed boundary (Q1). This is due to measurements at Q3 (orthogonal and linear regression-based data corrections) and Q4 (for linear regression-based data corrections only). The PM_{10} difference between Q1 and Q3 was also detected as significantly higher than the random scatter of inter-instrument PM_{10} differences for the linear regression-based data corrections, but not those adjusted using the orthogonal regressions.

The polar plots shown in Figure 5-8 indicate that on this day, that elevated levels of PM_{10} were shown by all monitors to be coming from offsite and from the northeast and southeast directions. It appears that Q1 was more impacted by these offsite sources than Q3 or Q4. The T640x polar plot for this day confirms that PM_{10} emissions from offsite sources impacted Q1 on this day, and so differences with other boundary monitors cannot be due to quarry activities.

It is therefore concluded that the quarry emissions did not result in an increase in PM_{10} of more than 2.5 µg/m^3 (24-hour average) on 10th November 2022.

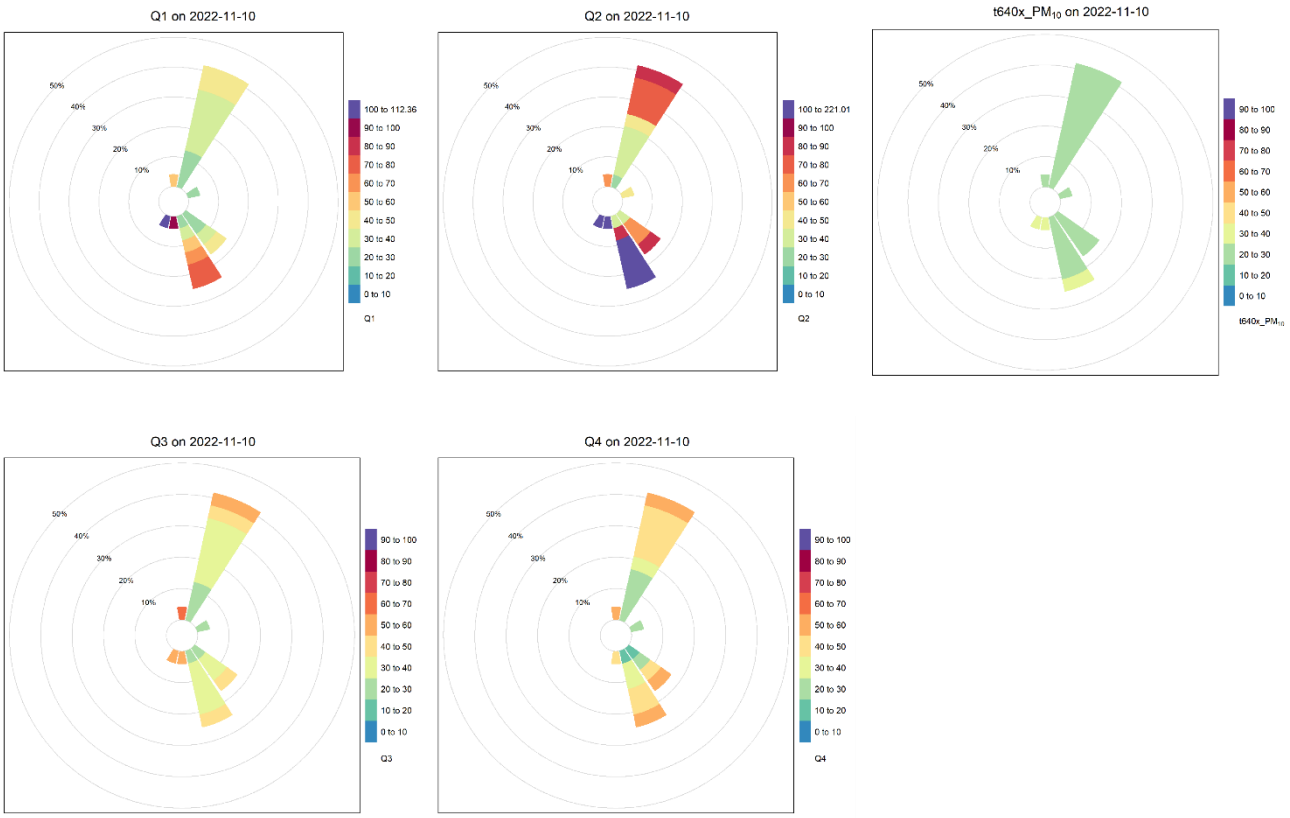

Figure 5.8: Polar plots for 1-hour Q1, Q2, Q3, Q4, T640x PM_{10} on 10/11/2022.

6.0 Discussion

The requirements to detect a 24-hour PM_{10} increase of as low as 2.5 µg/m^3 within the nearby Christchurch airshed that could be caused by quarrying activities is challenging and especially in an environment where there are a multitude of other dust generating sources surrounding the quarry.

To achieve effective compliance monitoring in this instance, the approach of co-locating real-time PM_{10} monitors to establish inter-instrument random error and bias was essential and allowed for the subsequent application of a multiple statistical test methods for detecting statistically significant increases in 24-hour PM_{10} between western/southern and the eastern boundaries of the site.

This statistical significance information combined with detailed analysis of hourly meteorological records and varying ambient particulate levels, has provided a sound approach for detecting increases in ambient PM_{10} due to quarrying activities and therefore the extent of compliance with related air discharge consent requirements.

The outcome of applying the above methods, has been the identification of other significant sources of ambient PM_{10} within the Templeton area, which stem from the direction of, agriculturally worked farmland, horse tracks and the nearby motorway. The presence of these sources means that compliance monitoring in this instance was challenging and there was a significant risk that the quarry activities could be incorrectly attributed to elevated ambient PM_{10} levels and equating these to non-

compliance with the air discharge consent for incremental 24-hour PM_{10} impacts within the neighbouring airshed.

On all occasions where the potential for non-compliance with the air discharge consent was detected, an inspection of bias due to fog events and the influence from offsite PM_{10} sources always found that these factors were the cause of apparent increases in ambient PM_{10} within the Christchurch airshed.

Whilst the routine was employed for removing sub-hourly PM_{10} monitoring data impacted by fog events, it is clear that this routine did not always avoid occurrences of potentially false positive findings of non-compliant increases in ambient 24-hour average PM_{10}. In all cases these potentially false positive results were successfully identified by drilling down into the hourly meteorological and particulate data for each day and for each monitor (i.e., those located at quarry boundaries and opposite the airshed boundary).

In summary, detailed monitoring methods and subsequent array of statistical approaches, and cross checking for offsite sources, have been employed for this compliance assessment. The result is that a reliable assessment of the quarry's compliance with Condition 29 of its air discharge consent has, in our view, been achieved.

7.0 Conclusion

Following the analysis of ambient respirable particulate monitoring data, which was collected at various site boundary locations during 2022 (before and during bund formation and other quarrying activities), it is concluded that the Roydon Quarry activities did not cause an increase of more than 2.5 µg/m^3 of 24-hour average PM_{10} within the nearby Christchurch airshed. Therefore, it is concluded that the site complied with Regulation 17(1) of the Resource Management (National Environmental Standards for Air Quality) Regulations 2004.

8.0 References

Aberkane, T. (2019). *Evaluation of PM Instruments in New Zealand.* Queenstown, New Zealand: CASANZ19.

McClosky, D., & Hagan, D. H. (2024). *Identifying and Removing Data Records Influenced by Fog. (2024.03).* https://doi.org/ 10.5281/zenodo.10793534.

Ministry for the Environment. (2009). *Good Practice Guide for Air Quality Monitoring and Data Management.* Wellington: Ministry for the Environment. Retrieved from https://www.mfe.govt.nz/sites/default/files/good-practice-guide-for-air-quality.pdf

Quant Modulair-PM Product Specification Sheet. (2022). Retrieved from Quant AQ website: https://assets.quant-aq.com/downloads/spec-sheets/modulair-pm.latest.pdf

Limitations

This Report is provided by Port Hill Limited ("PortHill") subject to the following limitations:

- This Report has been prepared for the specific purpose outlined in PortHill's proposal. No responsibility is accepted for the use of this Report, in whole or in part, in other contexts or for any other purpose.
- The scope and the period of PortHill's Services are as described in PortHill's proposal and are subject to restrictions and limitations. PortHill did not perform a complete assessment of all possible conditions or circumstances that may exist at the site referenced in the Report. If a service is not expressly indicated, do not assume it has been provided. If a matter is not addressed, do not assume that any determination has been made by PortHill in regard to it.
- Any assessments, designs, and advice provided in this Report are based on the conditions indicated from published sources and the investigation described. No warranty, express or implied, is included that the actual conditions will conform exactly to the assessments contained in this Report.
- Where data supplied by the client or other external sources have been used, it has been assumed that the information is correct unless otherwise stated. PortHill accepts no responsibility for incomplete or inaccurate data supplied by others.
- The Client acknowledges that PortHill may have retained subconsultants affiliated with PortHill to provide Services for the benefit of PortHill. PortHill will be fully responsible to the Client for the Services and work done by all its subconsultants and subcontractors. The Client agrees to assert claims and seek to recover losses, damages, or other liabilities only from PortHill and not from PortHill's affiliated companies. To the maximum extent allowed by law, the Client waives any expense, loss, claim, demand, or cause of action against PortHill's affiliated companies, and their employees, officers, and directors.
- This Report is provided for the sole use by the Client and is confidential to them. No responsibility whatsoever for the contents of this Report will be accepted to any person other than the Client. Any use by a third party, or reliance on or decisions based on this Report, is the responsibility of such third parties. PortHill accepts no responsibility for damages, if any, suffered by any third party as a result of decisions made or actions based on this Report.

Appendix A Monitoring Data Validation

1.0 Introduction

This appendix describes the process of preparing QuantAQ, T640x and meteorological monitoring data for analysis.

2.0 T640x

Raw 1-minute T640x data was first cleaned to remove readings during the calibration period. One-hour and 24-hour average values were then calculated when data capture rate was greater than 75% for that hour and 24-hour period respectively.

3.0 Meteorological data

Raw 15-minute meteorological data, including, temperature, relative humidity, rainfall, wind direction, wind speed, were converted to 1 hour and 24-hour averages when data capture rate was greater than 75% for each respective period.

4.0 QuantAQ

One-minute QuantAQ datasets were first cleaned to remove readings that are beyond the monitor's specifications, i.e., PM readings > 2000 µg/m^3 and RH > 95%. (Quant Modulair-PM Product Specification Sheet, 2022).

The QuantAQ dust monitors operate without heated inlets, making them susceptible to environmental conditions, such as high relative humidity. Without a heated inlet, moisture can condense on particles or within the monitor itself, which can lead to artificially elevated readings or fluctuations. The QuantAQ manufacturer has applied an internal correction factor to account for this known issue, similar to the approach described in Crilley et al., (2018).

However, a comparison of hourly QuantAQ and T640x data for the colocation period shows that QuantAQs have significantly elevated values on occasions. QuantAQ are undertaking research to develop a robust approach for fog identification, but in the meantime have published a method for identifying and removing data records influenced by fog.

The routine used for removing data records when fog interference is likely to be present is published by QuantAQ (McClosky & Hagan, 2024). This identifies fog events when 1-minute temperature data records indicate a wet bulb suppression <3.75°C (i.e., dry bulb – wet bulb < 3.75°C), and when combined with the coarse fraction of respirable particulate ($PM_{2.5-10}$) being > 200 µg/m^3 (based on the mid-point of a 11 minute rolling average). Wet bulb suppression is referred to as the dew point temperature spread by Quant (McClosky & Hagan, 2024). The method used for calculation of the wet bulb suppression is also published in this paper.

McClosky & Hagan (2024) note that this is a simple heuristic that can be applied post processing and the method proposed is temporary fix while more robust methods are being developed.

Figure 1 shows the 24-hour average PM10 during the colocation period for all monitors without fog removal, while Figure 2 shows the same with fog removal.

After the data was cleaned, 1-hour and 24-hour average values were calculated when data capture rate was greater than 75% for the period being considered.

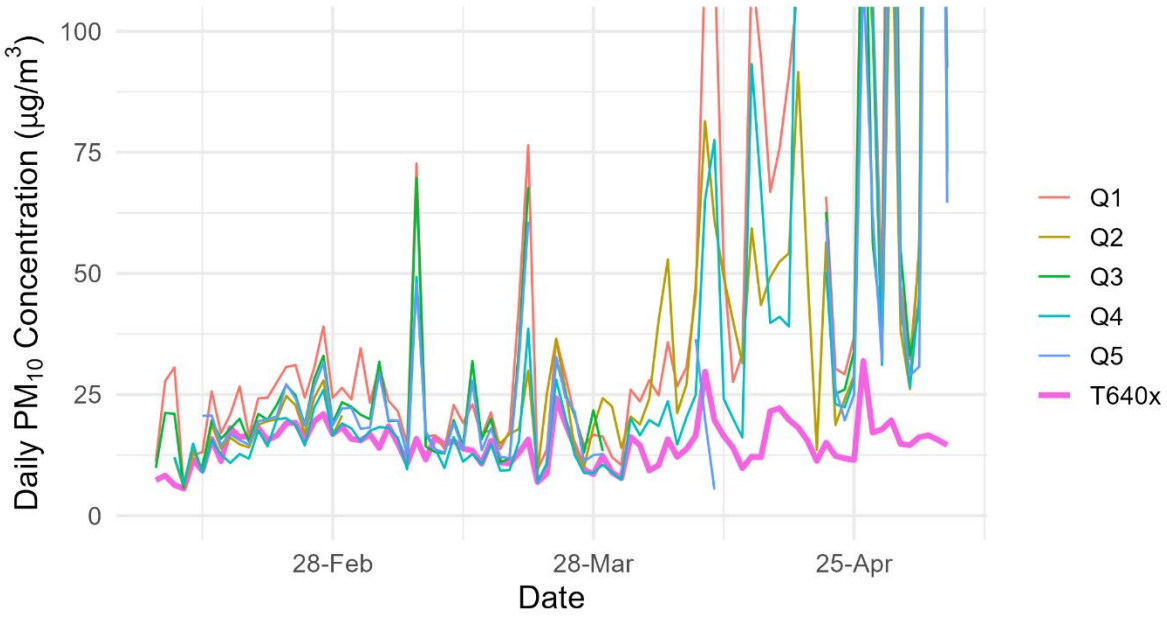

Figure 1: Timeseries of 24-hour average QuantAQ without fog removal and T640x data for the colocation period.

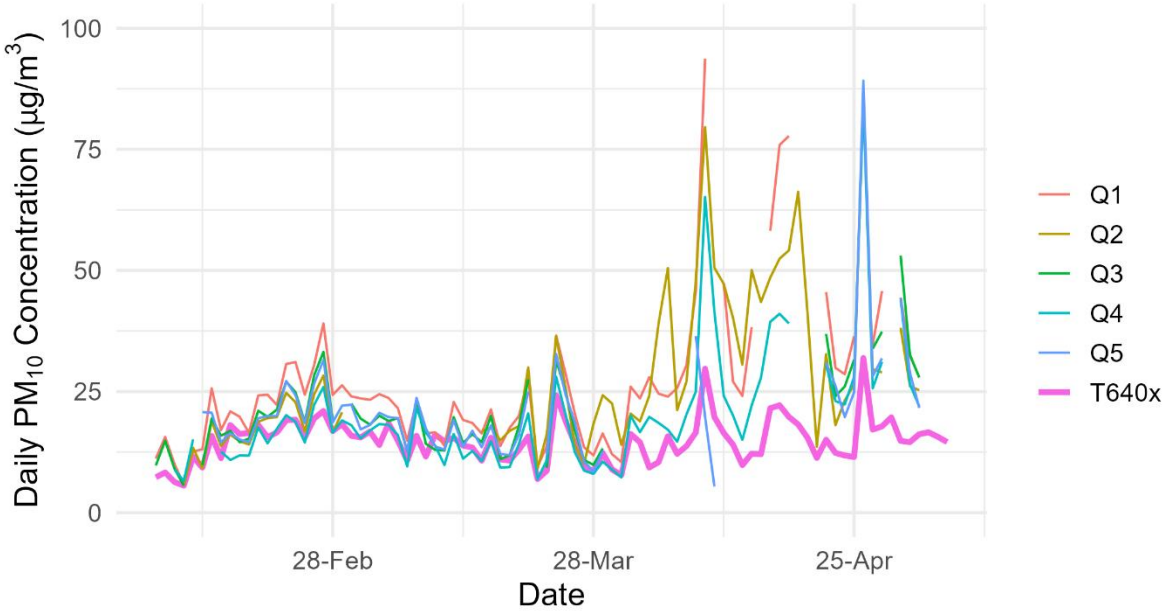

Figure 2: Timeseries of 24-hour average QuantAQ with fog removal and T640x data for the colocation period.

5.0 Data Capture Rate

Table 1 shows the data capture rate for 24-hour average PM_{10} without fog event removal during the colocation, background monitoring and bund formation periods, while Table 2 shows the same with fog removal. After fog events were removed, the data capture rates for QuantAQ monitors range from 85 % to 94 % for bund formation period.

Table 1: Data capture rate for 24-hr average concentrations during colocation, background monitoring and bund formation periods. Fog events were not removed for QuantAQ data.

Period	Total days	Q1 (PM_{10})	Q2 (PM_{10})	Q3 (PM_{10})	Q4 (PM_{10})	Q5 (PM_{10})	T640x (PM_{10})	Meteorological data (RH, temperature, wind speed, direction)
Colocation	86	98%	83%	71%	95%	72%	100%	100%
Background monitoring	62	100%	100%	100%	100%	98%	98%	100%
Bund formation	142	89%	94%	96%	93%	94%	99%	100%

Table 2: Data capture rate for 24-hr average concentrations during colocation, background monitoring and bund formation periods. Fog events were removed for QuantAQ data.

Period	Total days	Q1 (PM_{10})	Q2 (PM_{10})	Q3 (PM_{10})	Q4 (PM_{10})	Q5 (PM_{10})	T640x (PM_{10})	Meteorological data (RH, temperature, wind speed, direction)
Colocation	86	90%	79%	65%	88%	67%	100%	100%
Background monitoring	62	92%	89%	92%	92%	94%	98%	100%
Bund formation	142	85%	89%	94%	89%	93%	99%	100%

6.0 Paired 24-hour PM_{10} Comparison

Figure 3 shows a scatter plot of 24-hour averaged QuantAQ PM_{10} (without fog removal) compared to 24-hour averaged near reference monitor measurements during the colocation period, while Figure 4 shows the same with fog removal. It shows that without fog removal, there is a wide range of high outliers in the QuantAQ PM_{10} concentrations, as shown in Figure 3, while the data points in Figure 4 are more closely clustered, with fewer high outliers, which indicates stronger corelation.

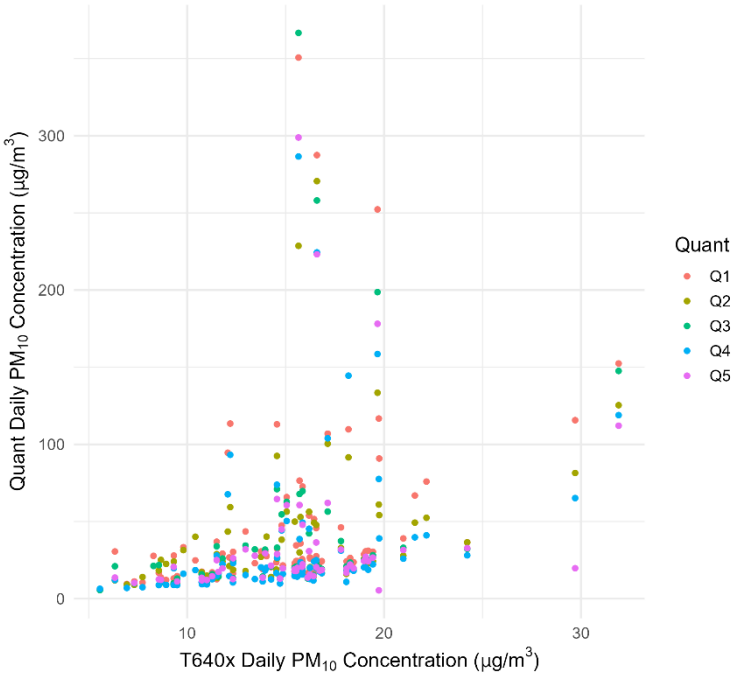

Figure 3: Paired 24-hour PM_{10} measured by QuantAQ Quant monitors (without fog removal) versus 24-hour measurements by T640x during colocation period.

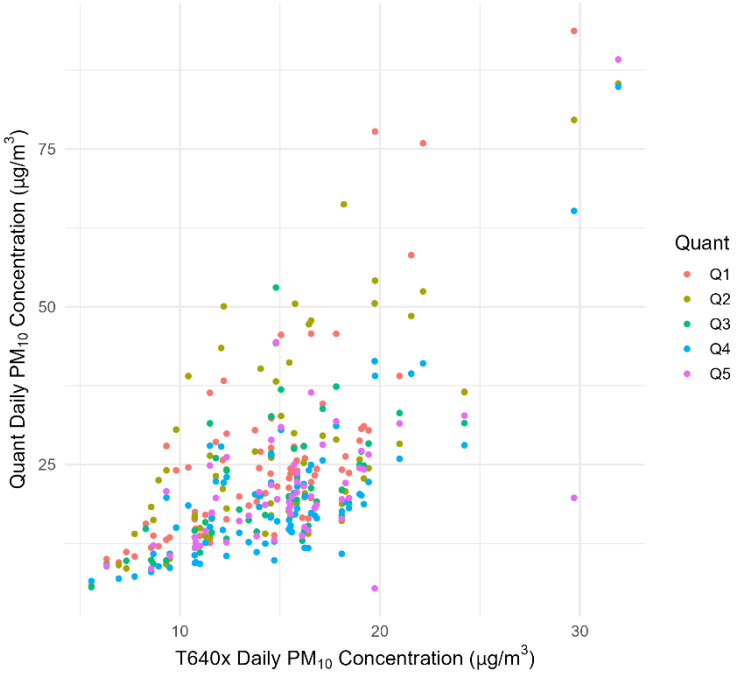

Figure 4: Paired 24-hour PM_{10} measured by QuantAQ Quant monitors (with fog removal) versus 24-hour measurements by T640x during colocation period.

7.0 Summary

In summary these results indicate that there is a stronger correlation after removal of PM_{10} data during fog events identified by the method developed by QuantAQ (McClosky & Hagan, 2024). This is confirmed during the development of regression equations in Appendix B.

8.0 References

Crilley, L. R., Shaw, M., Pound, R., Kramer, L. J., Price, R., Young, S., & Lewis, A. C. (2018). valuation of a Low-Cost Optical Particle Counter (Alphasense OPC-N2) . *Atmospheric Meas. Tech*, 11 (2), 709–720. .

McClosky, D., & Hagan, D. H. (2024). *Identifying and Removing Data Records Influenced by Fog. (2024.03)*. Retrieved from https://doi.org/ 10.5281/zenodo.10793534

Quant Modulair-PM Product Specification Sheet. (2022). Retrieved from Quant AQ website: https://assets.quant-aq.com/downloads/spec-sheets/modulair-pm.latest.pdf

Appendix B Data Correlation

1.0 Introduction

This appendix describes the process of developing correction factors for QuantAQ PM_{10} using the 24-hour averaged QuantAQ and T640x data.

2.0 Orthogonal Regression

Orthogonal regression is widely considered to be the most suitable model to establish the correlation between two measurements given that this regression accounts for inherent measurement errors or uncertainties in both the x and y variables.

This approach has been applied to QuantAQ monitors, utilising data both with and without fog removal to develop correction factors. For Q1 monitor, 24 hour averaged data collected for the whole monitoring period were used, while for other monitors, data from colocation period were used.

In this assessment, an uncertainty of 1.25 µg/m^3 was assumed for the T640x, consistent with the uncertainty value determined from its calibration against TEOM with FDMS using orthogonal regression, as reported by Aberkane (2019). It should be noted that in this compliance assessment, the T640x data has not been adjusted to align with an NES referenced method. Without adjustment, T640x PM_{10} data is generally higher than the PM_{10} measured from an NES method by approximately 10 % (Aberkane, 2019).

Table 1 summarises the correction factors for 24-hour averaged PM_{10} and the correlation coefficient (R^2) between the QuantAQ and T640x PM_{10}. It shows that the R^2 has improved when using the QuantAQ data with fog removal, but still ranges from 0.34 to 0.57, indicating this regression is not perfect.

Orthogonal regression was repeated using data adjusted using the correction factors in Table 1. Table 2 shows the equations established from adjusted data. It shows that for data with fog removal, the slope has significantly reduced, approaching a value to 1, while this trend was not observed in data without fog removal.

Before correction, the scatter plots of the 24-hour QuantAQ PM_{10} with and without fog removal, versus T640x 24-hour PM_{10} are shown in Figure 1 and Figure 2, respectively. After correction, the same data is shown in Figure 3 and Figure 4, respectively.

Timeseries of the adjusted 24-hour QuantAQ PM_{10} during the colocation period with T640x are shown in Figure 6. Figure 7 shows the timeseries of adjusted 24 hour Q1 PM_{10} during the whole monitoring period with T640x.

Table 1: Correction factors developed for 24 -hour QuantAQ data with and without fog removal – orthogonal regression.

QuantAQ Monitor	Correction Factor – without fog removal	Correction Factor – with fog removal
Q1	Q1c = Q1r / 24.1+ 14.07 R^2 = 0.07	Q1c = Q1r / 2.52+ 5.94 R^2 = 0.41
Q2	Q2c = Q2r / 24.06+ 13.19 R^2 = 0.14	Q2c = Q2r / 4.63+ 8.82 R^2 = 0.46
Q3	Q3c = Q3r / 45.67+ 13.93 R^2 = 0.09	Q3c = Q3r / 3.56+ 8.59 R^2 = 0.35
Q4	Q4c = Q4r / 30.81+ 13.86 R^2 = 0.11	Q4c = Q4r / 3.37+ 8.93 R^2 = 0.57
Q5	Q5c = Q5r / 46.72+ 14.65 R^2 = 0.05	Q5c = Q5r / 3.85+ 9.93 R^2 = 0.38

Table 2:.Equation established using adjusted QuantAQ data with and without fog removal – orthogonal regression.

QuantAQ Monitor	Equation after correction – without fog removal	Equation after correction – with fog removal
Q1	Q1c = Q1r / 0.07+ -201.84 R^2 = 0.07	Q1c = Q1r / 0.64+ -8.64 R^2 = 0.41
Q2	Q2c = Q2r / 0.16+ -77.08 R^2 = 0.14	Q2c = Q2r / 0.62+ -9.21 R^2 = 0.46
Q3	Q3c = Q3r / 0.1+ -132.77 R^2 = 0.09	Q3c = Q3r / 0.51+ -13.77 R^2 = 0.35
Q4	Q4c = Q4r / 0.12+ -110.61 R^2 = 0.11	Q4c = Q4r / 0.75+ -5.04 R^2 = 0.57
Q5	Q5c = Q5r / 0.06+ -247.83 R^2 = 0.05	Q5c = Q5r / 0.54+ -13.1 R^2 = 0.38

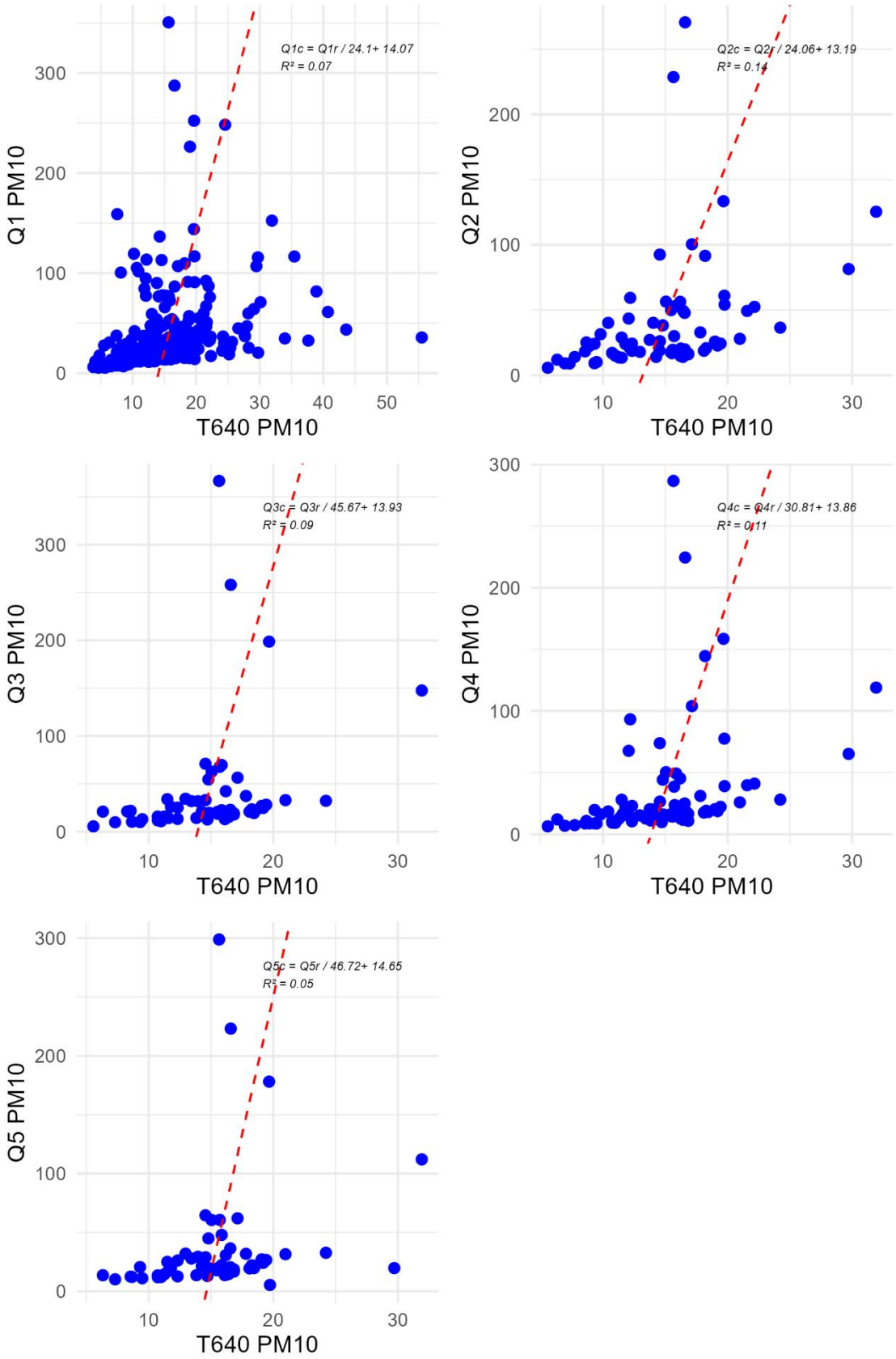

Figure 1: Scatter plots of 24 hour average QuantAQ PM_{10} (without fog removal) versus 24 hour T640x PM_{10}. Orthogonal regression is shown in these plots.

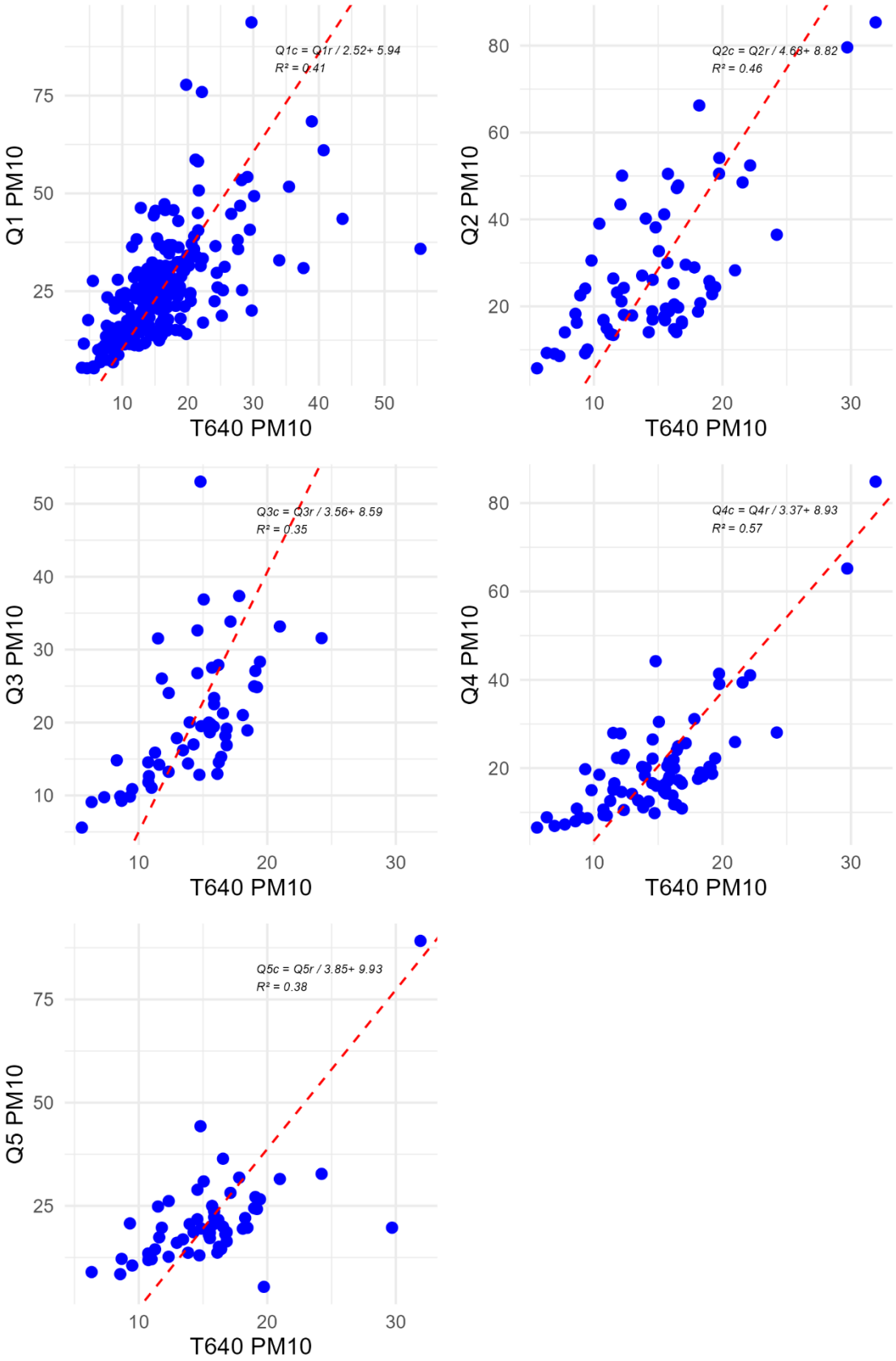

Figure 2: Scatter plots of 24 hour average QuantAQ PM_{10} (with fog removal) versus 24 hour T640x PM_{10}. Orthogonal regression is shown in these plots.

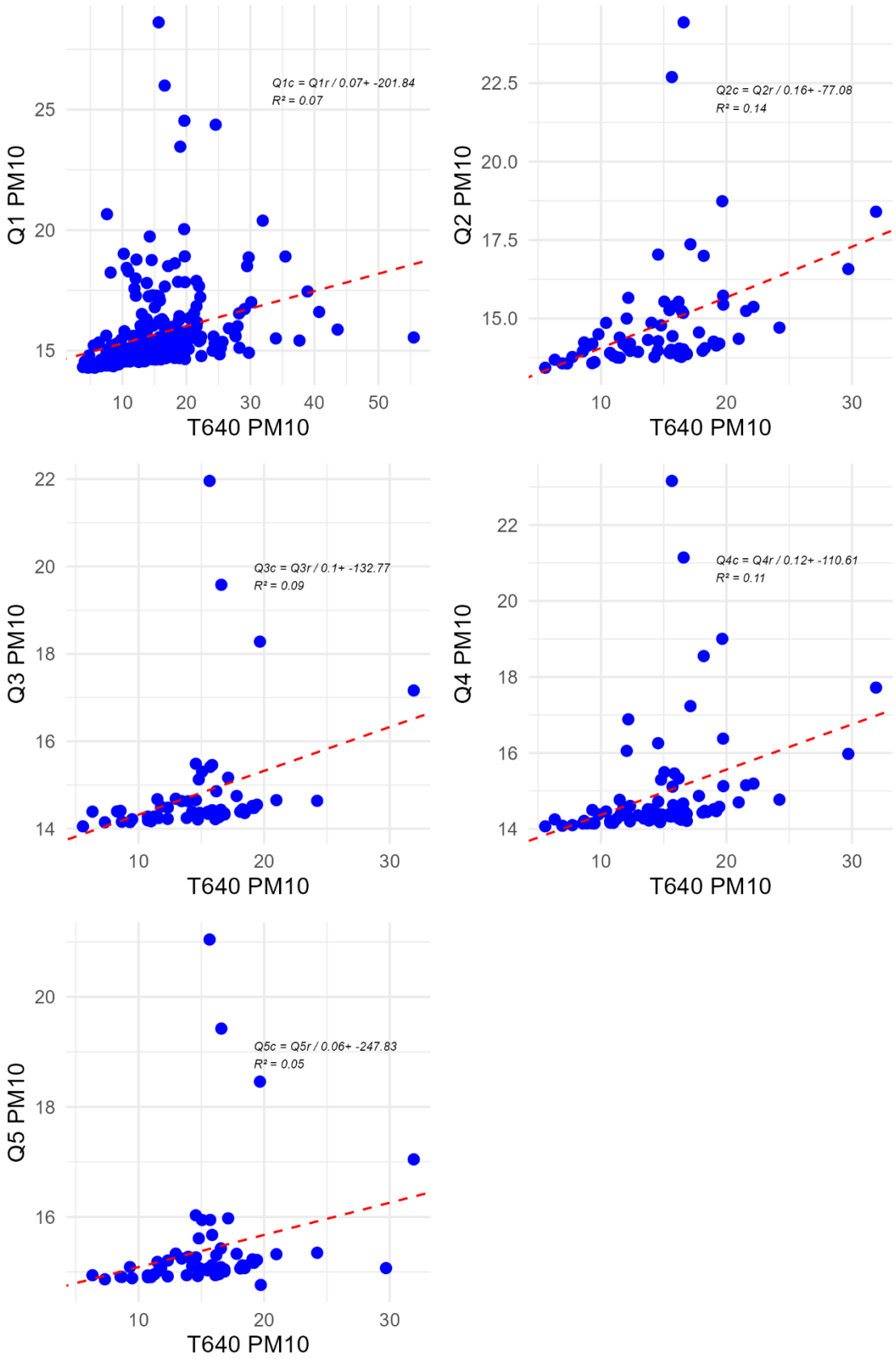

Figure 3: Scatter plots of adjusted 24 hour average QuantAQ PM_{10} (without fog removal) versus 24 hour T640x PM_{10}. Orthogonal regression is shown in these plots.

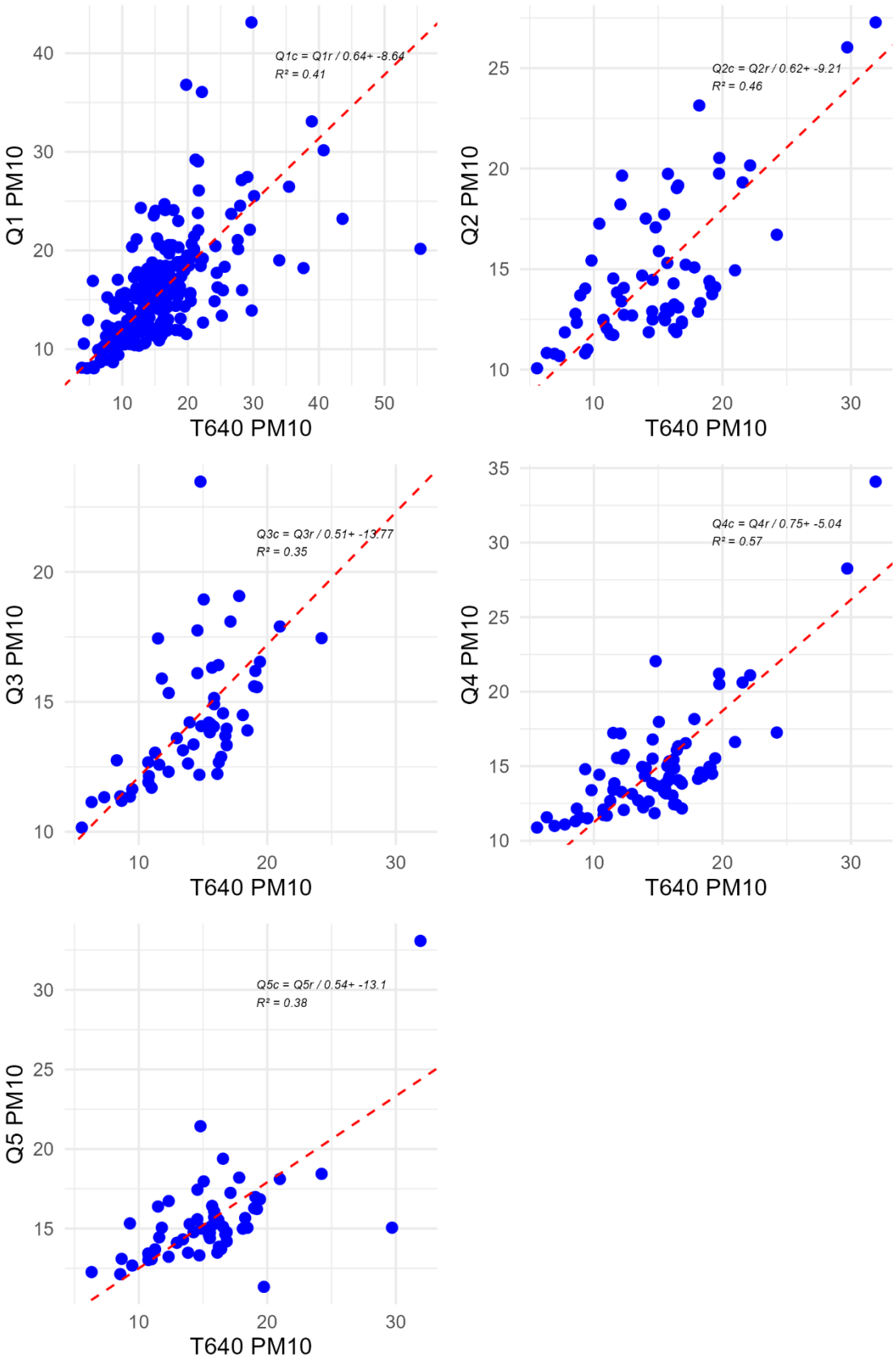

Figure 4: Scatter plots of adjusted 24 hour average QuantAQ PM_{10} (with fog removal) versus 24 hour T640x PM_{10}. Orthogonal regression is shown in these plots.

Based on the above analysis, QuantAQ data with fog removal has been selected for further analysis, as it significantly improves the regression outcomes. To assess the accuracy of the adjusted QuantAQ data relative to T640x during the colocation period, the mean absolute error (MAE) was calculated. The MAE provides a metric for the average magnitude of errors in the adjusted 24-hour QuantAQ PM_{10} , as presented in Table 3.

Table 3: Mean Absolute Error established between adjusted QuantAQ and T640x 24-hour PM_{10} during colocation period – orthogonal regression.

Monitor	MAE for 24-hour PM_{10} ($\mu g/m^3$)
Q1	3.4
Q2	3.1
Q3	2.5
Q4	2.5
Q5	2.6

The differences between the adjusted 24-hour QuantAQ data and the corresponding T640x data were compared against the 24-hour averaged relative humidity (RH) over the colocation period, as shown in Figure 5. Red lines in the figure represent the range of the corresponding mean absolute error (MAE). The plots suggest that at higher RH levels, some bias persists in the adjusted QuantAQ data.

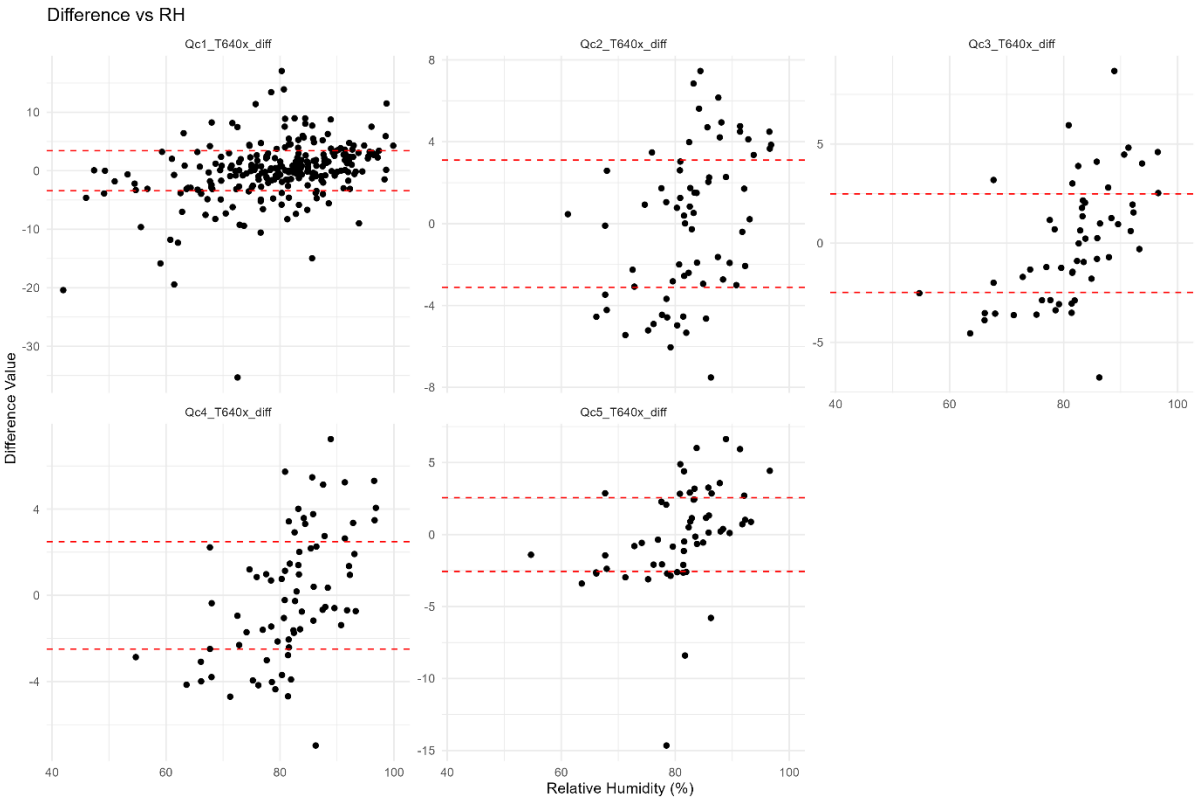

Figure 5: Scatter plots of differences between the adjusted 24 hour average QuantAQ PM_{10} (with fog removal) and T640x PM_{10} versus RH. The red lines indicate the corresponding MAE.

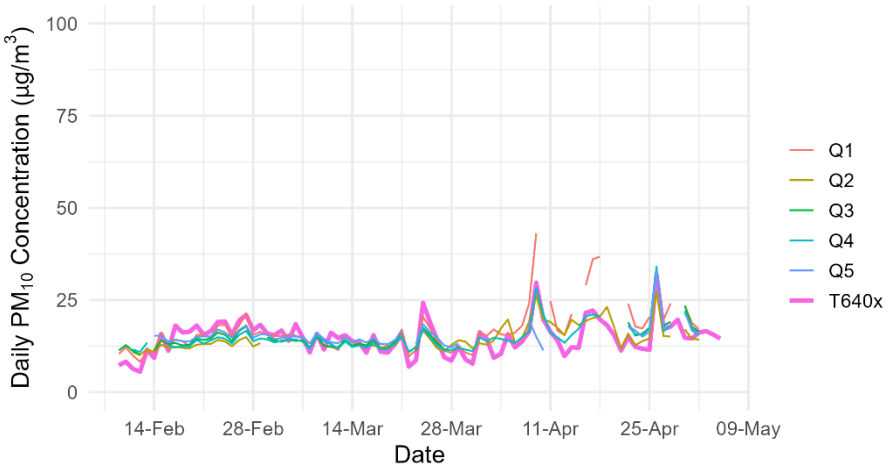

Figure 6: Timeseries of adjusted 24-hour QuantAQ PM_{10} during colocation period with T640x.

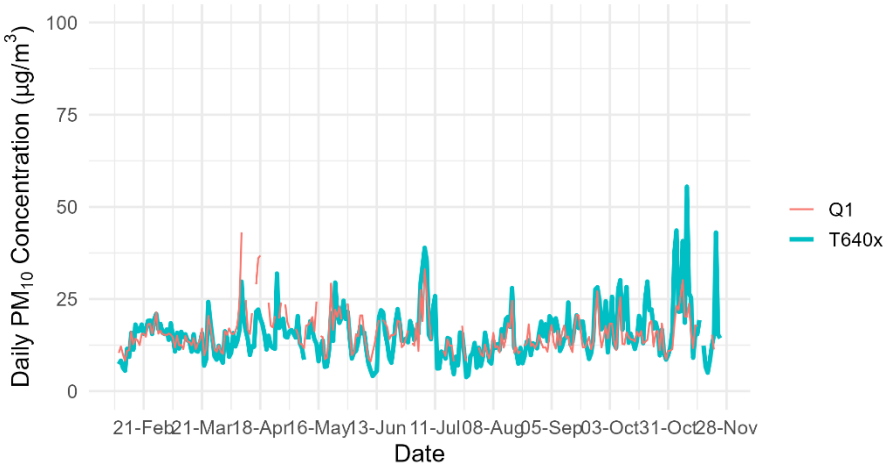

Figure 7: Timeseries of adjusted 24-hour Q1 PM_{10} for the whole monitoring period with T640x.

3.0 Multiple Linear Regression

Based on the orthogonal regression analysis, a multiple linear regression that incorporates RH was used to determine whether the correlation coefficient (R^2) improves when accounting for RH in the adjustment. QuantAQ data with fog removal has been used in this analysis.

Table 4 summarises these correction factors for 24-hour averaged PM_{10} and the correlation coefficient (R^2) between the QuantAQ and T640x PM_{10}. It shows that the R^2 ranges from 0.44 to 0.64, slightly improved over the orthogonal regression.

Multiple linear regression was then applied again to the adjusted data using the correction factors in Table 4. Table 5 shows the equations established from the adjusted data. It shows that for all monitors, the slopes to adjust the QuantAQ data and RH are 1 and 0 respectively, with the intercept closer to 0. R^2 has slightly increased for some monitors. These indicate improvement in correlation after the adjustment.

Figure 8 and Figure 9 show the scatter plots of the 24-hour QuantAQ PM_{10} versus T640x 24-hour PM_{10} before and after adjustment, respectively. The MAE statistics were calculated for the adjusted 24-hour QuantAQ PM_{10}, which is shown in Table 3.

Timeseries of the adjusted 24-hour QuantAQ PM_{10} during the colocation period with T640x are shown in Figure 10. Figure 11 shows the timeseries of adjusted 24 hour Q1 PM_{10} during the whole monitoring period with T640x.

The differences between the adjusted 24-hour QuantAQ data and the corresponding T640x data were compared against the 24-hour averaged relative humidity (RH) over the colocation period, as shown in Figure 12. This indicates that the uncertainties remain when humidity is high.

Table 4: Correction factors developed for 24 -hour QuantAQ data with fog removal – linear regression.

QuantAQ Monitor	Correction factors	Correlation coefficient (R^2)
Q1	Q1c = (Q1r - 0.28 * RH) / 1.31 + 14.07	0.47
Q2	Q2c = (Q2r - 0.36 * RH) / 2.45 + 15.8	0.49
Q3	Q3c = (Q3r - 0.34 * RH) / 1.73 + 18.78	0.44
Q4	Q4c = (Q4r - 0.43 * RH) / 2.32 + 21.29	0.64
Q5	Q5c = (Q5r - 0.39 * RH) / 1.76 + 21.42	0.45

Table 5: Correction factors developed for adjusted 24 -hour QuantAQ data with fog removal – linear regression.

QuantAQ Monitor	Correction factors	Correlation coefficient (R^2)
Q1	Q1c = (Q1r - 0 * RH) / 1 + -0.03	0.47
Q2	Q2c = (Q2r - 0 * RH) / 1 + -0.02	0.52
Q3	Q3c = (Q3r - 0 * RH) / 1 + -0.03	0.49
Q4	Q4c = (Q4r - 0 * RH) / 1 + 0.03	0.67
Q5	Q5c = (Q5r - 0 * RH) / 1 + 0.01	0.45

Table 6: Mean Absolute Error established between adjusted QuantAQ and T640x 24-hour PM_{10} during colocation period – linear regression.

QuantAQ Monitor	MAE for 24-hour PM_{10} ($\mu g/m^3$)
Q1	4.8
Q2	4.0
Q3	2.4
Q4	2.5
Q5	2.8

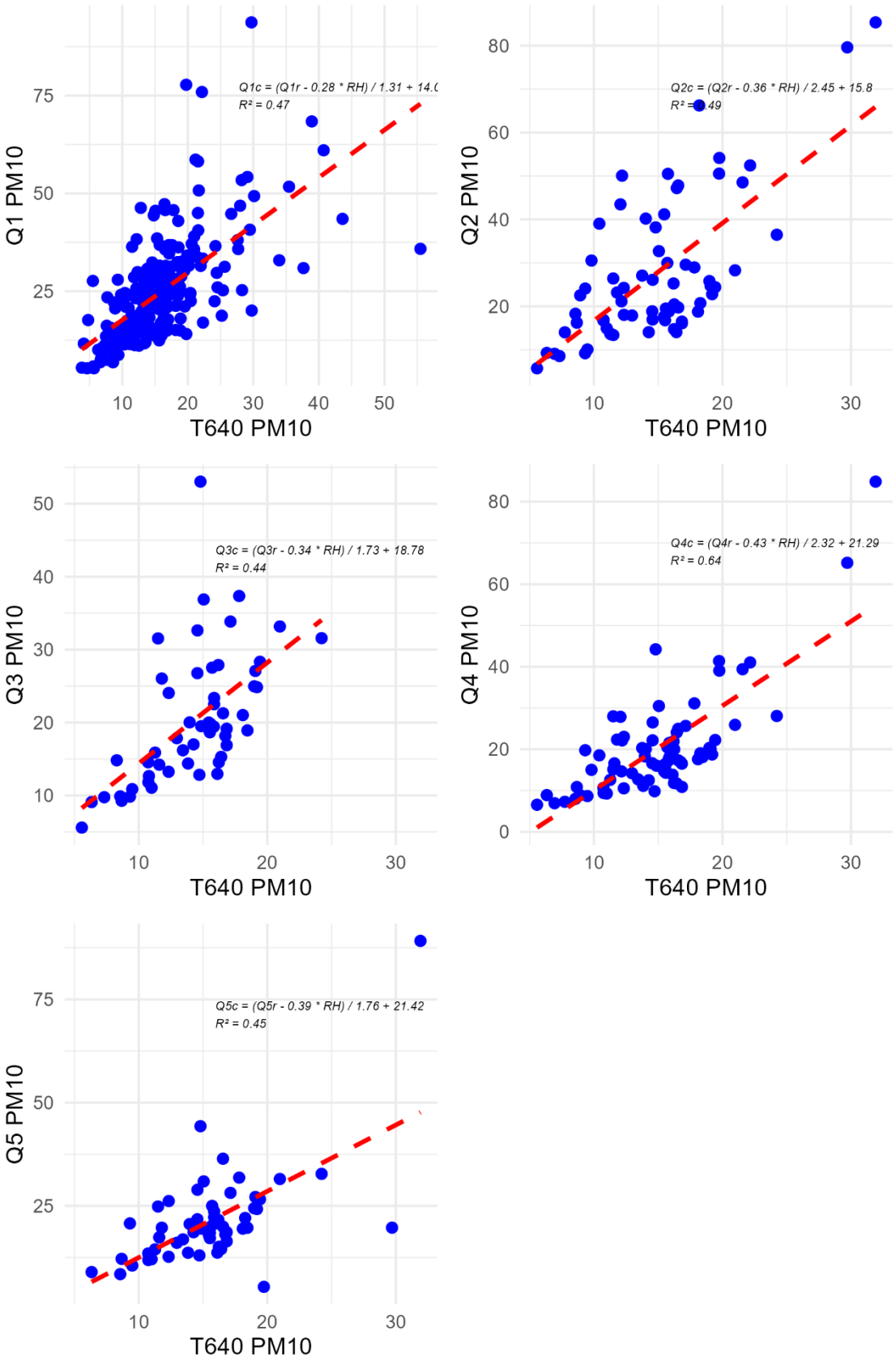

Figure 8: Scatter plots of unadjusted 24 hour average QuantAQ PM_{10} (with fog removal) versus 24 hour T640x PM_{10}. Multiple linear regression is shown in these plots.

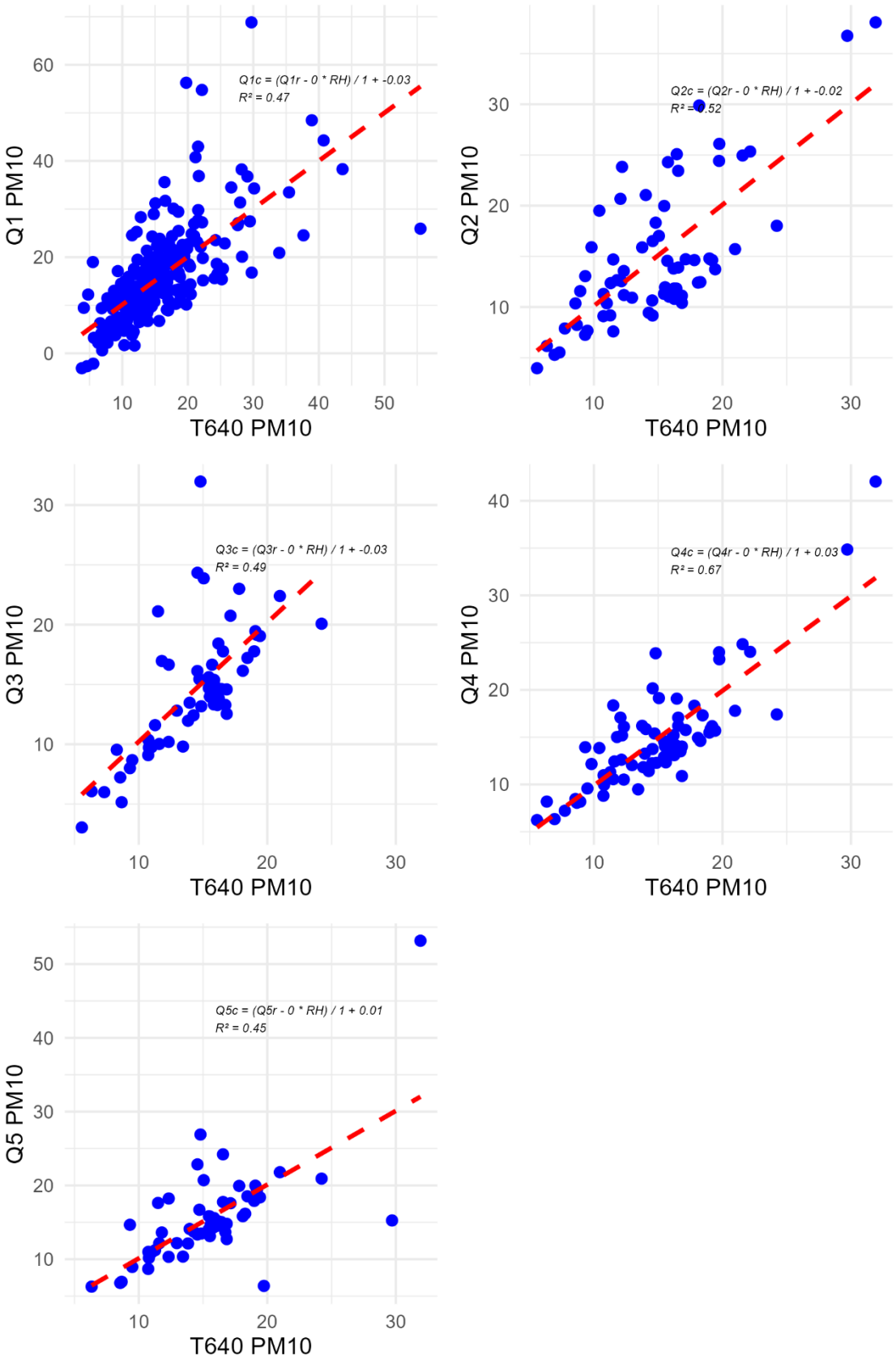

Figure 9: Scatter plots of adjusted 24 hour average QuantAQ PM_{10} (with fog removal) versus 24 hour T640x PM_{10}. Multiple linear regression is shown in these plots.

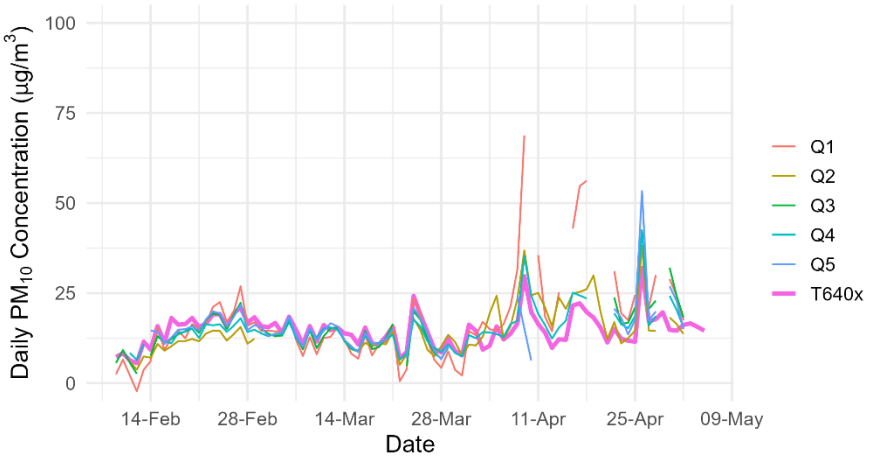

Figure 10: Timeseries of adjusted (linear regression) 24-hour QuantAQ PM_{10} during colocation period with T640x.

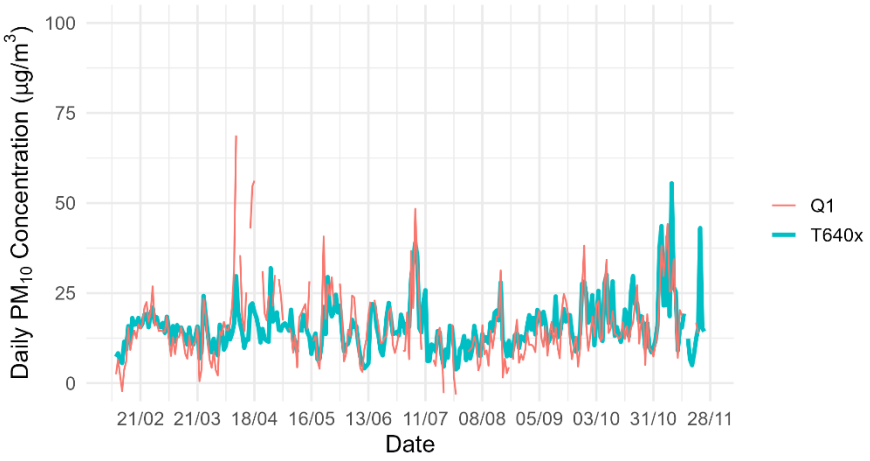

Figure 11: Timeseries of adjusted 24-hour Q1 PM_{10} for the whole monitoring period with T640x.

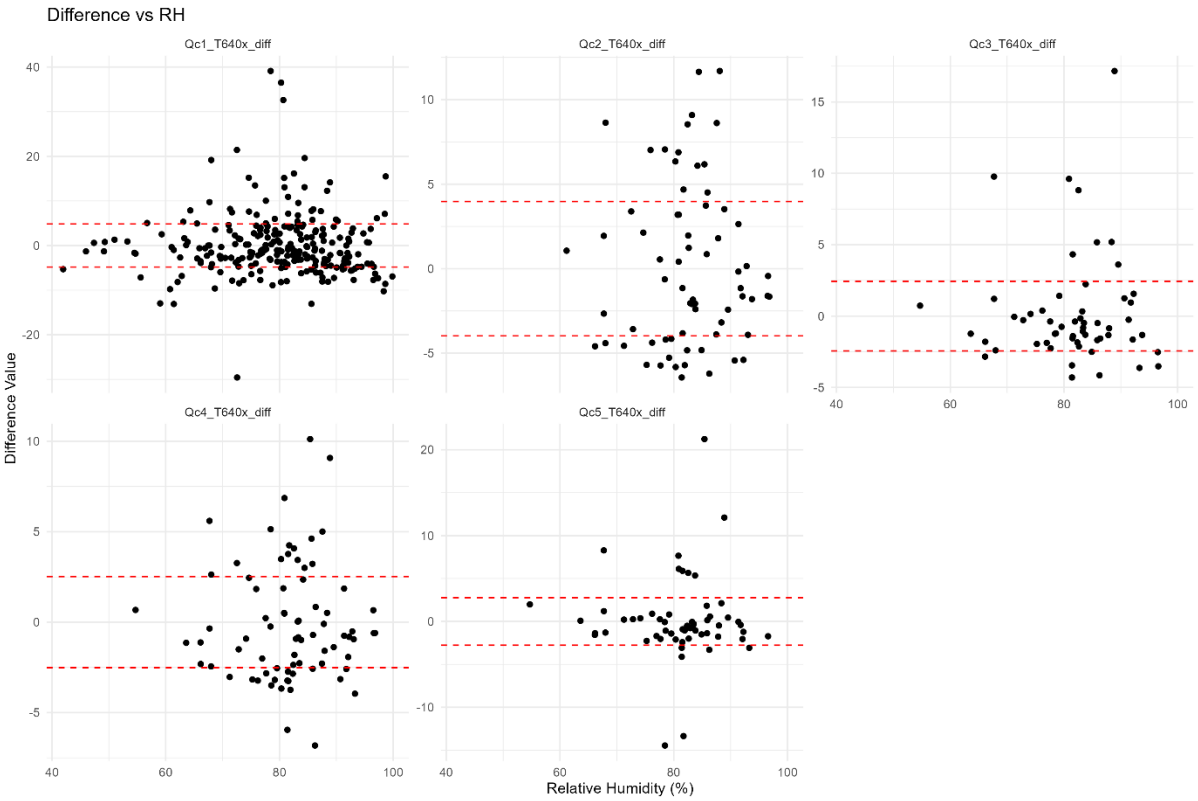

Figure 12: Scatter plots of differences between the adjusted 24 hour average QuantAQ PM_{10} (using linear regression) and T640x PM_{10} versus RH. The red lines indicate the corresponding MAE.

4.0 References

Aberkane, T. (2019). Evaluation of PM Instruments in New Zealand. *CASANZ19.* Queenstown, New Zealand.

Crilley, L. R., Shaw, M., Pound, R., Kramer, L. J., Price, R., Young, S., & Lewis, A. C. (2018). valuation of a Low-Cost Optical Particle Counter (Alphasense OPC-N2) . *Atmospheric Meas. Tech*, 11 (2), 709–720. .

McClosky, D., & Hagan, D. H. (2024). *Identifying and Removing Data Records Influenced by Fog. (2024.03).* Retrieved from https://doi.org/ 10.5281/zenodo.10793534

Appendix C Error and Statistical Analysis

1.0 Introduction

This appendix outlines the significance criteria (i.e. combine mean absolute error and 90th percentile upper confidence limit) derived from the error and statistical analyses.

2.0 Error Analysis

Mean absolute error (MAE) values for 24-hour PM_{10} concentrations were established for each QuantAQ monitor (Q1, Q2, Q3 and Q4) relative to the co-located T640x values, using both linear and orthogonal regression. These error values are presented in Table 1.

Combined MAE values were then developed for the paired differences in 24-hour PM_{10} concentrations measured between upwind and downwind QuantAQ monitors, i.e., (Q1 differences to Q2, Q3, and Q4), as shown in Table 2. The combined MAEs (based on linear and orthogonal regression adjusted data) were subsequently compared to the differences in 24-hour PM_{10} concentrations measured by Q1 and other QuantAQ monitors when placed at different locations during the monitoring period.

Table 1: Mean Absolute Error established between adjusted QuantAQ and T640x 24-hour PM10.

Monitor	MAE for 24-hour PM_{10} (µg/m^3)	
	Orthogonal regression	Linear regression
Q1	3.4	4.8
Q2	3.1	4.0
Q3	2.5	2.4
Q4	2.5	2.5
Q5	2.6	2.8

Table 2: Combined Mean Absolute Error for 24-hour QuantAQ PM_{10}.

Monitor	Combined MAE (µg/m^3)	Combined MAE (µg/m^3)
	Orthogonal regression	Linear regression
Q1 & Q2	4.6	6.3
Q1 & Q3	4.2	5.5
Q1 & Q4	4.2	5.4

3.0 Distribution of QuantAQ PM_{10} differences

The differences of 24-hour PM_{10} (µg/m^3) for the paired QuantAQ monitors were established using 24-hour PM_{10} concentrations measured during the co-location period. For the QuantAQ monitors, these were adjusted by linear and orthogonal regressions with the T640x results. The histograms of the distribution of these differences are shown in Figure 1.

Two statistical tests, Shapiro-Wilk (S-W) test and Kologorov- Smirnov (K-S) tests, were undertaken to confirm the non-normality or normality of these concentration difference distributions. The results are summarised in

Table 3, which indicates that when taking a S-W test, all of these differences are skewed distributed. By comparison, the K-S test indicates that the measured concentration differences of Q1 – Q4 are skewed distributed, but the differences of other monitors are normally distributed.

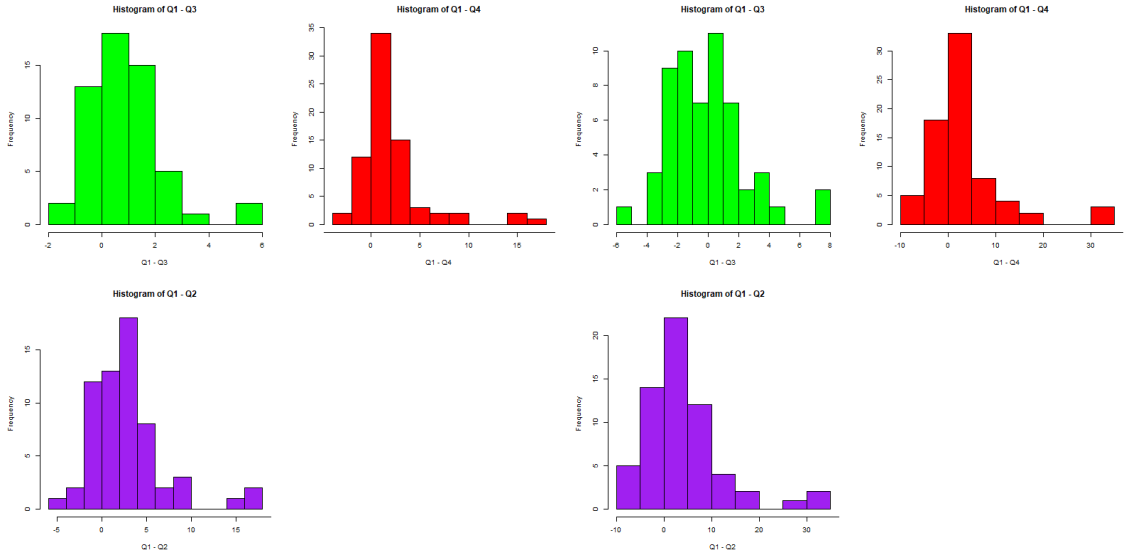

(data adjusted from orthogonal T640x regression) *(data adjusted from linear T640x regression)*

Figure 1: Histograms of the distribution of the paired QuantAQ monitors differences. The left figure was established from data adjusted by orthogonal regression. The right one was from data adjusted by linear regression.

Table 3: Statistical tests for differences distributions.

Difference	Adjusted from orthogonal regression		Adjusted from linear regression	
	S-W test	K-S tests	S-W test	K-S tests
Q1 – Q2	Skewed	Normal	Skewed	Normal
Q1 – Q3	Skewed	Skewed	Skewed	Skewed
Q1 – Q4	Skewed	Normal	Skewed	Normal

4.0 90th percentile Confidence Limit

The standard z-statistic, percentile and bootstrap methods were used to calculate the 90th percentile confidence limit for each difference distribution.

The standard z-statistic method assumes that the data is normally distributed and uses the mean and standard deviation of the data to estimate the confidence limits. For a 90th percentile confidence level, the z-value is approximately 1.28. The 90th percentile upper confidence limit is calculated as 90th percentile upper limit = mean ± (z × Standard deviation).

The percentile method does not assume normality and instead directly uses the data's empirical distribution. The data is sorted in ascending order, and the value at the 90th percentile is selected.

The bootstrap method is a resampling technique used to estimate the confidence limit without making assumptions about the data's distribution. This assessment takes a large number of random samples from each difference data, then the 90th percentile value was calculated for each resample. This process was then repeated for 10,000 times to create a distribution of the 90th percentiles as the 90th percentile upper confidence limit.

The results of these methods are summarised in Table 4 and Table 5. These show that the percentile methods provided the most conservative upper confidence limit, and these results are very similar to the z-statistic method. Bootstrap provides the highest values among these three methods.

Table 4: 90th percentile confidence limit for difference data adjusted from orthogonal regression.

Differences	90th percentile confidence limit (µg/m^3)		
	Standard z-statistic	Percentile	Bootstrap
Q1-Q2	-2.5 to 8.2	-1.5 to 6.4	4.5 to15.2
Q1-Q3	-0.9 to 2.6	-0.5 to 2.6	1.6 to 3.5
Q1-Q4	-2.3 to 6.7	-0.7 to 5.9	3.1 to 8.6

Table 5: 90th percentile confidence limit for difference data adjusted from linear regression.

Differences	90th percentile confidence limit (µg/m^3)		
	Standard z-statistic	Percentile	Bootstrap
Q1-Q2	7 to15	-5 to 11	7.9 to 28
Q1-Q3	-3.2 to 3	-3 to 3	1.4 to 4.6
Q1-Q4	-7 to 13	-4 to 11	5.5 to 18

admin@port-hill.com

PORTHILL